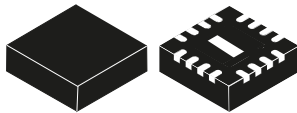


38 V, 10 W synchronous iso-buck converter for isolated applications



QFN16 (3 x 3 mm)

Maturity status link

[L6983I](#)

Features

- Designed for iso-buck topology
- 3.5 V to 38 V operating input voltage
- Primary output voltage regulation / no optocoupler required
- 4.5 A source / sink peak primary current capability
- Peak current mode architecture in forced PWM operation
- 390 ns blanking time
- 200 kHz to 1 MHz programmable switching frequency. Stable with low ESR capacitor: min 2 μ F
- Internal compensation network
- 2 μ A shutdown current
- Internal soft-start
- Enable
- Overvoltage protection
- Output voltage sequencing
- Thermal protection
- Optional spread spectrum for improved EMC
- Power Good
- Synchronization to external clock
- QFN16 (3x3 mm) package

Applications

- Isolated IGBT/SiC MOSFET gate drive supply
- OBC (On-board charger) for HEV/EV
- Electric traction systems

Description

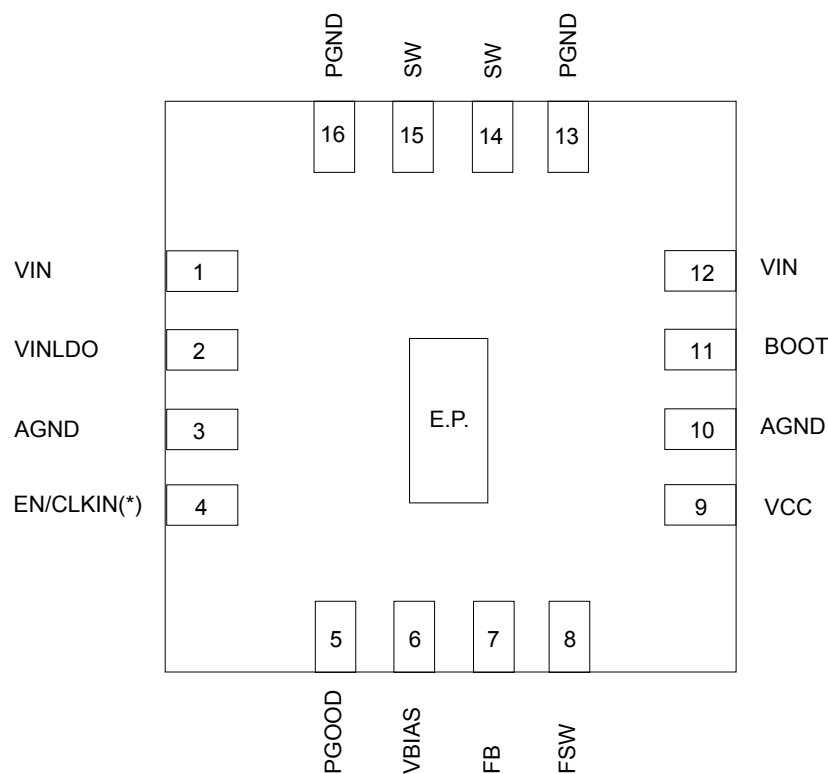
The **L6983I** is a device specifically designed for isolated buck topology. The primary output voltage can be accurately adjusted, whereas the isolated secondary output is derived by using a given transformer ratio. No optocoupler is required. The primary sink capability up to -4.5 A (even during soft-start) allows a proper energy transfer to the secondary side as well as enabling a tracked soft-start of the secondary output. The control loop is based on a peak current mode architecture and the device operates in forced PWM. The 390 ns blanking time filters oscillations, generated by the transformer leakage inductance, making the solution more robust.

The compact QFN16 3x3 mm package and the internal compensation of the **L6983I** help minimize design complexity and size.

The switching frequency can be programmed in the 200 kHz - 1 MHz range with optional spread spectrum for improved EMC. The EN pin provides enable/disable functionality.

The typical shutdown current is 2 μ A when disabled. As soon as the EN pin is pulled up the device is enabled and the internal 1.3 ms soft-start takes place. The **L6983I** features Power Good open collector that monitors the FB voltage. Pulse by pulse current sensing on both power elements implements an effective constant current protection and thermal shutdown prevents thermal run-away.

1 Pin configuration

Figure 1. Pin connection (top view)

Table 1. Pin description

Pin n°	Symbol	Function
1	VIN	DC input voltage
2	VINLDO	DC input voltage connects to the supply rail with a simple RC filter.
3	AGND	Analog ground
4	EN / CLKIN	Enable pin with internal voltage divider. Pull down/up to disable/enable the device. This pin is also used to provide an external clock signal, which synchronizes the device.
5	PGOOD	The PGOOD open collector output is driven to low impedance when the output voltage is out of regulation and released once the output voltage becomes valid.
6	VBIAS	Typically connected to the regulated output voltage, an external voltage source can be used to supply part of the analog circuitry to reduce current consumptions at light load. Connect to AGND if not used.
7	FB	FB is output voltage sensing with external voltage divider.
8	FSW	Connect an external resistor to program the oscillator frequency and enable optional dithering.
9	VCC	This pin supplies the embedded analog circuitry. Connect a ceramic capacitor ($\geq 1 \mu\text{F}$) to filter internal voltage reference.
10	AGND	Analog ground

Pin n°	Symbol	Function
11	BOOT	Connect an external capacitor (100 nF typ.) between BOOT and SW pins. The gate charge required to drive the internal nMOS is refreshed during the low-side switch conduction time.
12	VIN	DC input voltage
13	PGND	Power ground
14	SW	Switching node
15	SW	Switching node
16	PGND	Power ground
-	Exposed PAD	Exposed pad must be connect to AGND, PGND.

2 Typical application circuit

Figure 2. Basic application

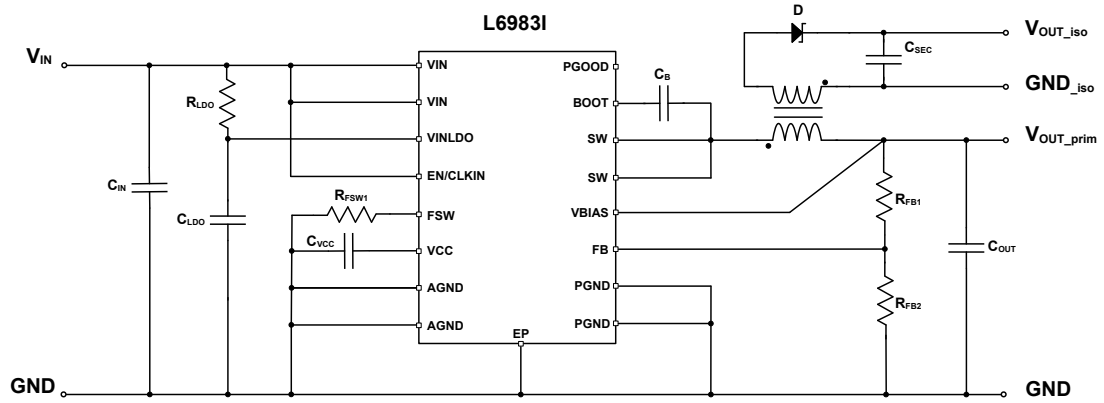


Table 2. Typical application component

Symbol	Value	Description	Note
C_{IN}	10 μ F	Input capacitor	
R_{LDO}	0.1 K Ω	VINLDO filter resistor	
C_{LDO}	1 μ F	VINLDO filter capacitor	
C_{VCC}	1 μ F	VCC bypass capacitor	
C_B	100 nF	Bootstrap capacitor	
C_{OUT}	3x22 μ F	Output capacitor	
R_{FB1}	400 K Ω	VOUT divider upper resistor	
R_{FB2}	82 K Ω	VOUT divider lower resistor	
R_{FSW1}	0 Ω	Frequency setting resistor	

3 Maximum ratings

3.1 Absolute maximum ratings

Stressing the device above the ratings listed in Table 3. Absolute maximum ratings may cause permanent damage to the device. These are stress ratings only and operation of the device at these or any other conditions above those indicated in the operating sections of this specification is not implied. Exposure to absolute maximum rating conditions may affect device reliability.

Table 3. Absolute maximum ratings

Symbol	Parameter	Min.	Max.	Unit
V_{IN}	Maximum pin voltage	-0.3	42	V
AGND	Maximum pin voltage	0	0	V
PGND	Maximum pin voltage	-0.3	0.3	V
BOOT	Maximum pin voltage	SW - 0.3	SW + 4	V
VCC	Maximum pin voltage	-0.3	Min. ($V_{IN} + 0.3$ V; 4 V	V
FB	Maximum pin voltage	-0.3	8	V
FSW	Maximum pin voltage	-0.3	VCC + 0.3	V
VBIAS	Maximum pin voltage	-0.3	$V_{IN} + 0.3$	V
EN	Maximum pin voltage	-0.3	$V_{IN} + 0.3$	V
PGOOD	Maximum pin voltage	-0.3	$V_{IN} + 0.3$	V
SW	Maximum pin voltage	-0.85	$V_{IN} + 0.3$	V
		-3.8 for 0.5 ns ⁽¹⁾		V
T_J	Operating temperature range	-40	150	°C
T_{STG}	Storage temperature range	-65	150	°C
T_{LEAD}	Lead temperature (soldering 10 sec.)		260	°C
$I_{HS, ILS}$	High-side / low-side RMS switch current		3	A

1. Negative peak voltage during switching activities caused by parasitic layout elements.

3.2 ESD protection

Table 4. ESD performance

Symbol	Parameter	Test conditions	Value	Unit
ESD	ESD protection voltage	HBM	2	kV
		CDM (corner pins)	750	V
		CDM	500	

3.3 Thermal characteristics

Table 5. Thermal data

Symbol	Parameter	Package	Value	Unit
R_{th_JA}	Thermal resistance junction ambient (device soldered on the STMicroelectronics demonstration board, please refer to Section 11 Application board)	QFN16	42	°C/W

4 Electrical characteristics

$T_J = 25\text{ °C}$, $V_{IN} = 12\text{ V}$ unless otherwise specified.

Table 6. Electrical characteristics

Symbol	Parameter	Test conditions	Min.	Typ.	Max.	Unit
V_{IN}	Operating input voltage range		3.5		38	V
V_{INH}	V_{CC} rising threshold		2.3		3.3	V
V_{INL}	V_{CC} UVLO falling threshold		2.15		3.15	V
$I_{PK}^{(1)}$	Peak current limit	Duty cycle < 40%	4.1	4.6		A
		Duty cycle = 99%. Closed loop operation	3.1	3.6		A
I_{VY}	Valley current limit		3.3	3.9	4.6	A
$I_{VY_SINK}^{(1)}$	Reverse current limit	V_{OUT} overvoltage	4	4.5	5	A
R_{DSON_HS}	High-side RDSON			0.130		Ω
R_{DSON_LS}	Low-side RDSON			0.085		Ω
T_{OFF_MIN}	Minimum off-time			200		ns
T_{ON_MIN}	Minimum on-time		330	390	450	ns
Enable						
V_{WAKE_UP}	Wake-up threshold	Rising			0.7	V
		Falling	0.2			V
V_{EN}	Enable threshold	Rising	1.08	1.2	1.32	V
		Hysteresis		0.2		V
V_{CC} regulator						
V_{CC}	LDO output voltage		3.0	3.3	3.6	V
Power consumption						
I_{SHTDWN}	Shutdown current from V_{IN}	$V_{EN} = GND$		2	3	μA
I_{Q_VIN}	Quiescent current from V_{IN}	$V_{BIAS} = GND$	1.6	2.3	3	mA
		$V_{BIAS} = 5\text{ V}$	300	550	800	μA
I_{Q_VBIAS}	Quiescent current from V_{BIAS}	$V_{BIAS} = 5\text{ V}$	1.3	1.8	2.3	μA
Soft-start						
T_{SS}	Internal soft-start		1	1.3	1.6	ms
Error amplifier						
V_{FB}	Voltage feedback	$-40\text{ °C} \leq T_J \leq 125\text{ °C}^{(2)}$	0.845	0.85	0.855	V
Overvoltage protection						
V_{OVP}	Overvoltage trip (VOVP/VREF)		115	120	125	%
V_{OVP_HYST}	Overvoltage hysteresis		1	2	6	%
Synchronization						
f_{CLKIN}	Synchronization range		200		1000	kHz
V_{CLKIN_TH}	Amplitude of synchronization clock		2.3			V

Symbol	Parameter	Test conditions	Min.	Typ.	Max.	Unit
$V_{\text{CLKIN_T}}^{(3)}$	Synchronization pulse ON and OFF-time $2.3 \leq V_{\text{CLKIN_TH}} \leq 2.5$ V	$V_{\text{CLKIN_TH}} = 2.3$ V	60			ns
	Synchronization pulse ON and OFF-time $V_{\text{CLKIN_TH}} > 2.5$ V		20			ns
Power good						
V_{THR}	PGOOD threshold	$-40\text{ }^{\circ}\text{C} \leq T_{\text{J}} \leq 125\text{ }^{\circ}\text{C}^{(2)}$	87	90	93	%
$V_{\text{THR_HYST}}$	PGOOD hysteresis (QFN version only)			3		
V_{PGOOD}	PGOOD open collector output	$V_{\text{IN}} > V_{\text{INH}}$ and $V_{\text{FB}} < V_{\text{TH}}$ 4 mA sinking load			0.4	V
		$2 < V_{\text{IN}} < V_{\text{INH}}$ 4 mA sinking load			0.8	V
$T_{\text{SHDWN}}^{(3)}$	Thermal shutdown temperature			165		$^{\circ}\text{C}$
$T_{\text{HYS}}^{(3)}$	Thermal shutdown hysteresis			30		$^{\circ}\text{C}$

1. Parameter tested in the static condition during testing phase. The parameter value may change over a dynamic application condition.
2. Specifications in the -40 to $125\text{ }^{\circ}\text{C}$ temperature range are assured by characterization and statistical correlation.
3. Not tested in production.

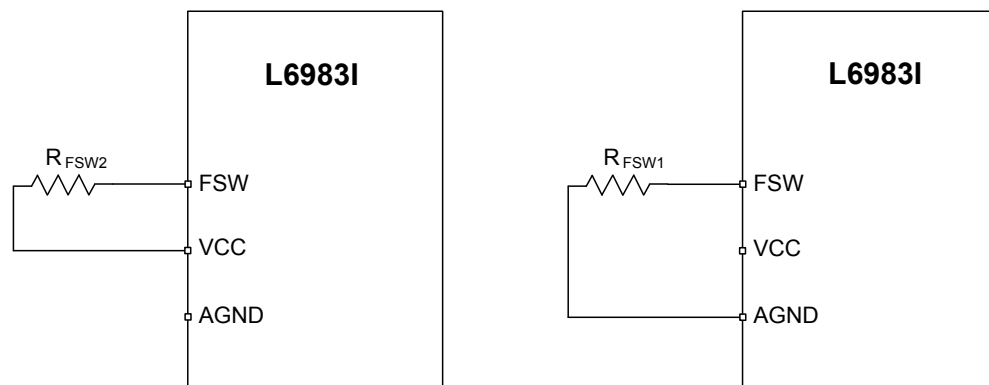
4.1 Frequency selection table

All the populations tested at $T_J = 25\text{ }^\circ\text{C}$, $V_{IN} = 12\text{ V}$ unless otherwise specified.

Table 7. FSW selection

Symbol	Option	RFSW1 (k Ω)	RFSW2 (K Ω)	Min.	Typ.	Max.	Unit
F _{sw}	Dithering	1.8	N.C.		200		kHz
		0	N.C.		400		kHz
		3.3	N.C.		500		kHz
		5.6	N.C.		700		kHz
		10	N.C.		1000		kHz
	No dithering	N.C.	1.8		200		kHz
		N.C.	0	360	400	440	kHz
		N.C.	3.3		500		kHz
		N.C.	5.6	630	700	770	kHz
		N.C.	10	900	1000	1100	kHz

Figure 3. Frequency setting with dithering (left) and without (right)

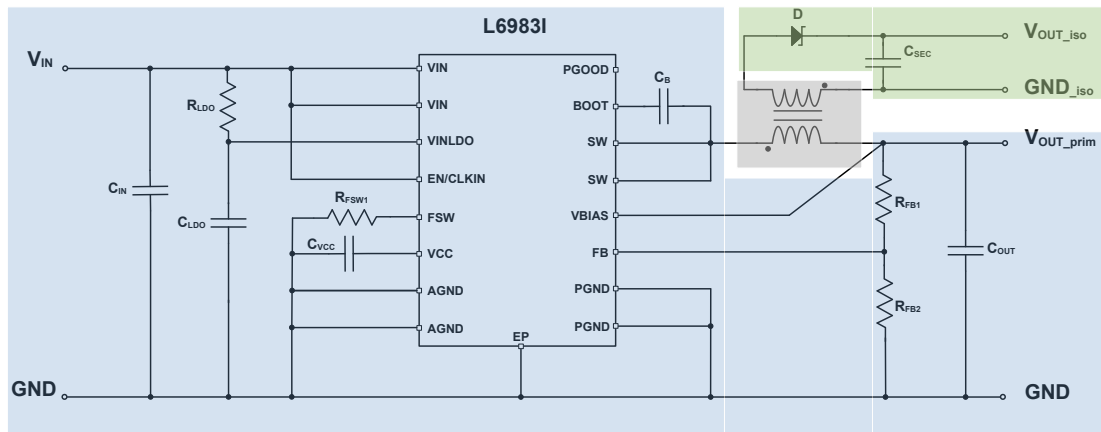


5 Functional description

The iso-buck topology based on the L6983I consists of:

- Primary side, the regulation loop of the peak current mode architecture regulates the primary voltage (blue area in the image below)
- A two-windings transformer (in gray)
- The secondary side, which generates the isolated output voltage (in green) given the selected transformer ratio.

Figure 4. Iso-buck general schematic



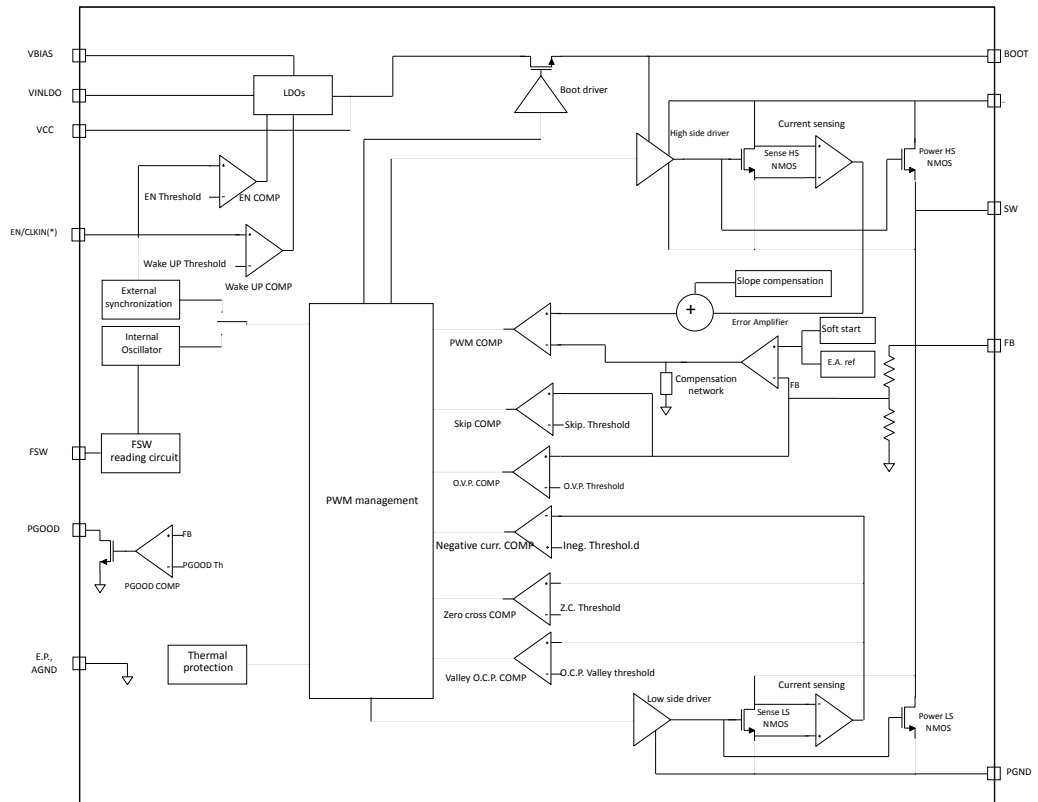
5.1 Primary side

The L6983I device is based on a “peak current mode” architecture with constant frequency control. Therefore, the intersection between the error amplifier output and the sensed inductor current generates the PWM control signal to drive the power switch.

The device operates in forced PWM control, allowing negative currents to flow in the synchronous MOSFET, hence transferring energy to the secondary coil during the off-time.

The main internal blocks shown in Figure 5 :

- Embedded power elements
- A fully integrated adjustable oscillator, which is able to set five different switching frequencies from 200 kHz to 1 MHz
- The ramp for the slope compensation avoiding subharmonic instability
- A transconductance error amplifier with integrated compensation network
- The high-side current sense amplifier to sense the inductor current
- A “Pulse Width Modulator” (PWM) comparator and the driving circuitry of the embedded power elements
- The soft-start block ramps up the reference voltage on error amplifier thus decreasing the inrush current at power-up. The EN pin inhibits the device when driven low
- The EN/CLK pin section, which allows synchronizing the device to an external clock generator
- The pulse-by-pulse high-side / low-side switch current sensing to implement the constant current protection
- A circuit to implement the thermal protection function
- The OVP circuitry to discharge the output capacitor in case of overvoltage event
- The switchover capability of the internal regulator to supply a portion of the quiescent current when the VBIAS pin is connected to an external output voltage
- Enable / disable dithering operation.

Figure 5. Block diagram


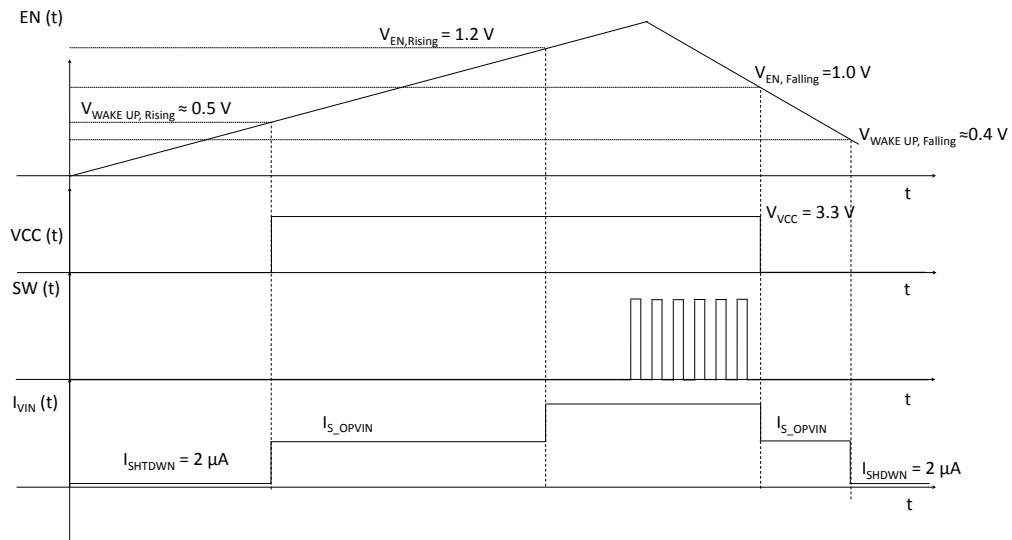
5.1.1 Enable

The EN pin is a digital input that turns the device on or off.

In order to maximize both the EN threshold accuracy and the current consumption, the device implements two different thresholds:

1. The Wake-up threshold, $V_{WAKE_UP} = 0.5\text{ V}$ (see [Section 4 Electrical characteristics](#)).
2. The Start-up threshold, $V_{EN} = 1.2\text{ V}$ (see [Section 4 Electrical characteristics](#).) The following image shows the device behavior.

Figure 6. Power-up/down procedure



When the voltage applied on the EN pin rises over $V_{WAKEUP\ THR, RISING}$, the device powers up the internal circuit increasing the current consumption.

As soon as the voltage rises over $V_{ENTHR, RISING}$, the device starts the switching activities as described in [Section 5.1.2 Soft-start](#).

Once the voltage becomes lower than $V_{ENTHR, FALLING}$, the device interrupts the switching activities.

As soon as the voltage becomes lower than $V_{WAKEUP\ THR.FALLING}$, the device powers down the internal circuit reducing the current consumption.

The pin is V_{IN} compatible.

Please refer to [Table 6. Electrical characteristics](#) for the reported thresholds.

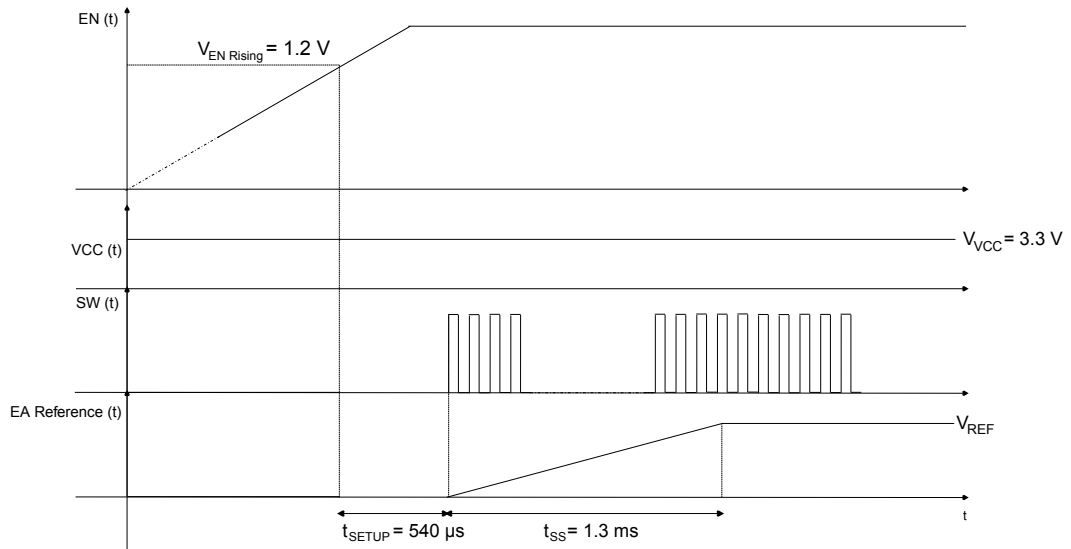
5.1.2 Soft-start

The soft-start (SS) limits the inrush current surge and makes the output voltage increase monotonically.

The device implements the soft-start phase ramping the internal reference with very small steps. Once the SS ends the error amplifier reference is switched to the internal value of 0.85 V coming directly from the band gap cell.

The soft-start duration is fixed and has a typical value of 1.3 ms.

Figure 7. Soft-start procedure

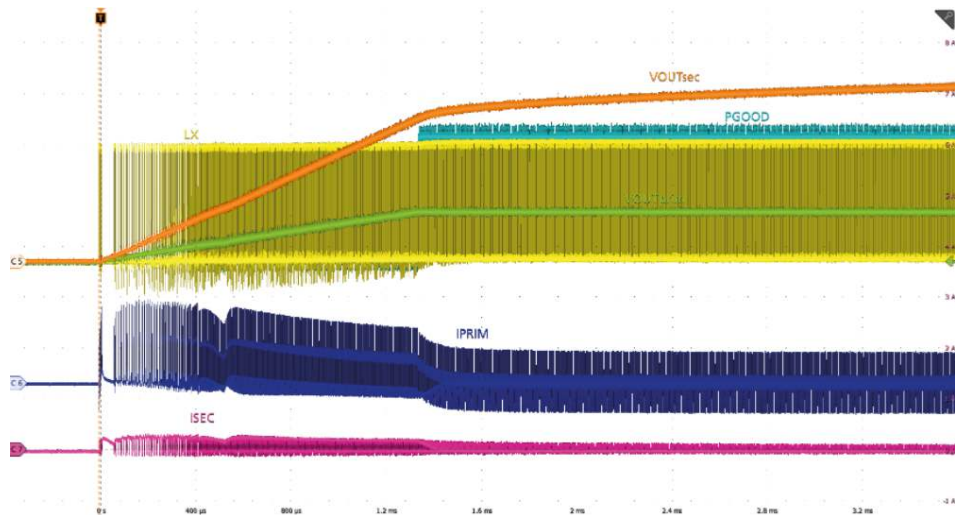


During normal operation, a new soft-start cycle takes place in case of:

1. Thermal shutdown event
2. UVLO event
3. EN pin rising over VEN threshold. Please refer to [Table 6. Electrical characteristics](#)

The device can invert the current even during soft-start, hence enabling the energy transfer to the secondary winding. Therefore, the secondary isolated output voltage goes up simultaneously with the primary output voltage, so implementing a tracked soft-start.

Figure 8. Tracked soft-start at secondary side



5.1.3 Undervoltage lockout

The device implements the undervoltage lockout (UVLO) continuously sensing the voltage on the V_{CC} pin, if the UVLO lasts more than 10 μs, the internal logic resets the device by turning off both LS and HS.

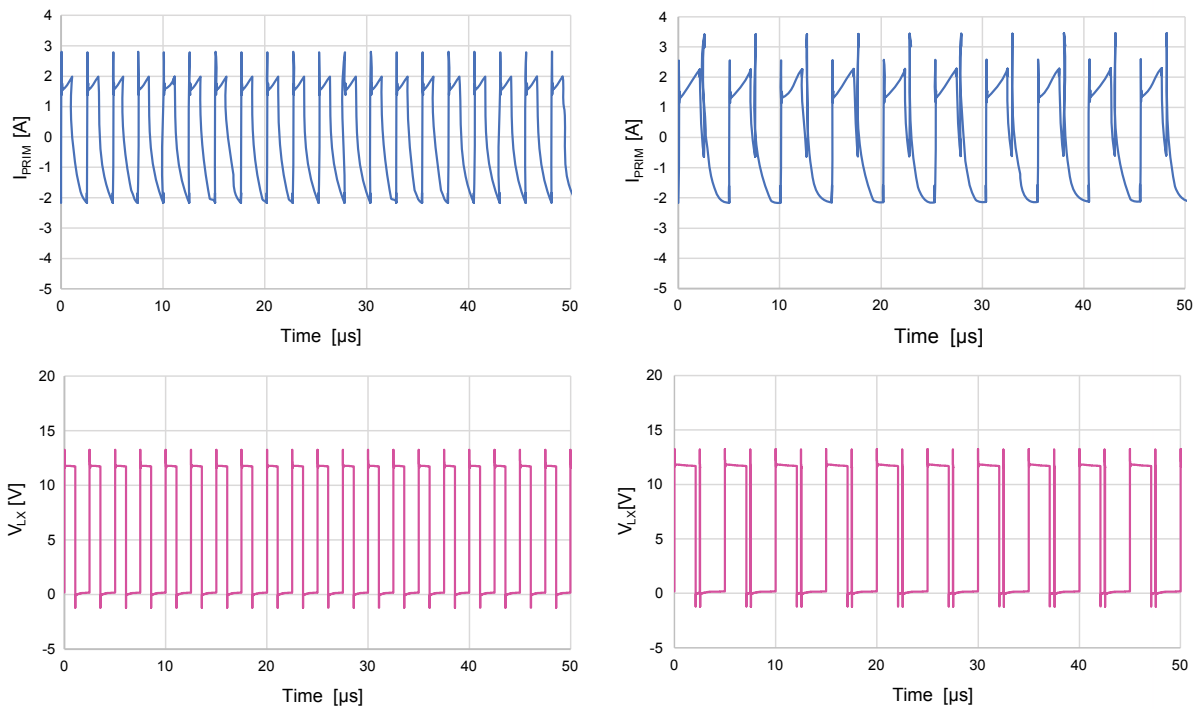
After the reset, if the EN pin is still high, the device repeats the soft-start procedure.

5.1.4 Minimum on-time

The current sense in the high-side MOSFET is not active (masked) for a certain time at the beginning to the on-time (masking time, from which the parameter $T_{ON\ MIN}$ derives).

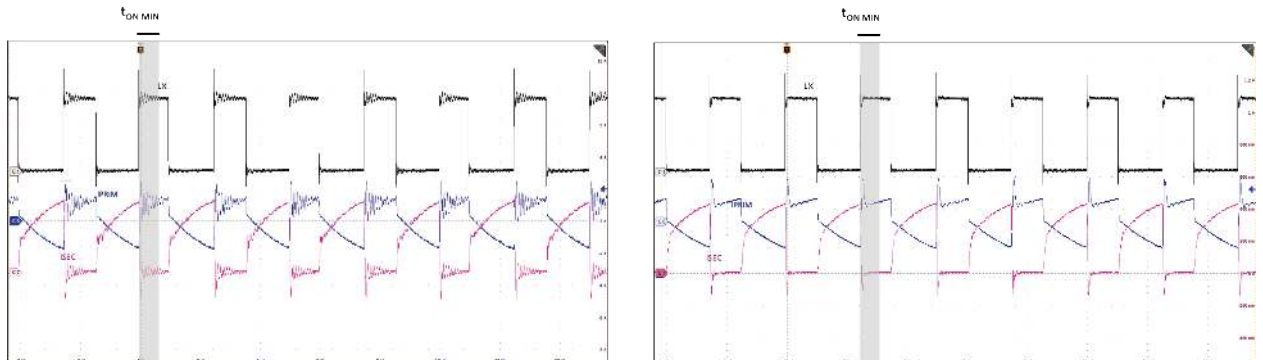
This current sense blanking time is implemented to prevent any primary side pulsed current at the high-side turn-on (resonating with transformer leakage inductance, parasitic capacitances, reverse junction capacitance of the Schottky diode of the secondary side) from overcoming the EA programmed switch current for the conversion, which would make the conversion unstable (depicted in Figure 9). For the L69831, the $T_{ON\ MIN}$ has a typical value of 390 ns.

Figure 9. Simulation with different masking times: insufficient (< 100 ns, left) and appropriate (390 ns, right)



Despite the masking time, an RC snubber (for example, across the Schottky diode of the secondary side) is normally recommended to damp oscillations. Figure 10 shows how the RC snubber helps in smothering the remaining oscillations.

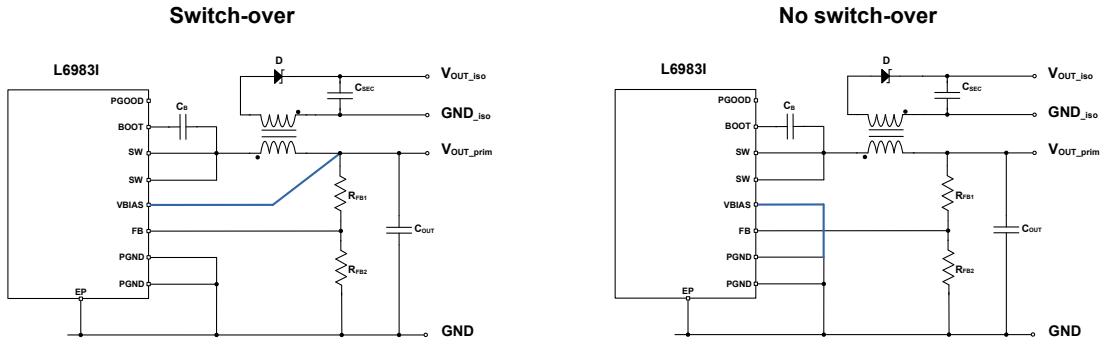
Figure 10. Remaining oscillations (left) and their filtering with RC snubber (right) $V_{IN} = 12\text{ V}$, $N = 6$, $I_{OUT\ Iso} = 200\text{ mA}$



5.1.5 Switch-over feature

The switch-over (selectable by connecting the VBIAS pin as shown in Figure 11, left) helps to improve the efficiency, especially at lower currents.

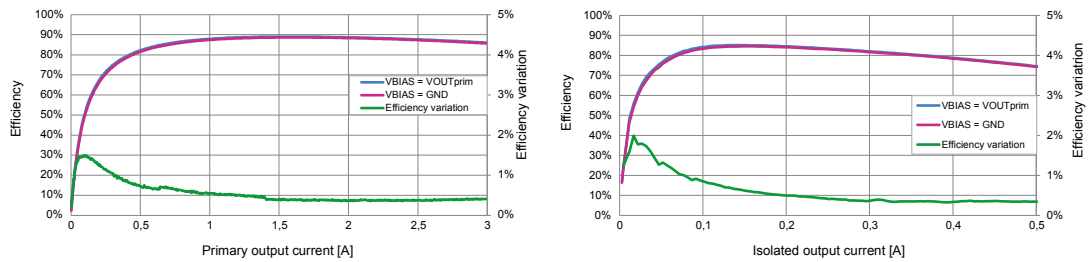
Figure 11. Switch-over selection



VBIAS can be also connected to an external power supply. The external power supply connected to the VBIAS pin must be disabled when the voltage on the EN pin is lower than V_WAKE_UP.

The effect on the efficiency for both the primary output and the secondary isolated output are shown in Figure 12.

Figure 12. Effect of the switch-over on the efficiency for primary output (left) and isolated secondary output (right)



5.1.6 Spread spectrum

The spread spectrum feature, helpful to improve EMC performances, is selectable by connecting the RFSW resistor to the VCC pin (please refer to Section 4.1 Frequency selection table). The internal dithering circuit changes the switching frequency in a range of $\pm 5\%$.

$$\Delta F_{SW} = 10\% \cdot F_{SW} \quad (1)$$

The device updates the frequency every clock period by fixed steps:

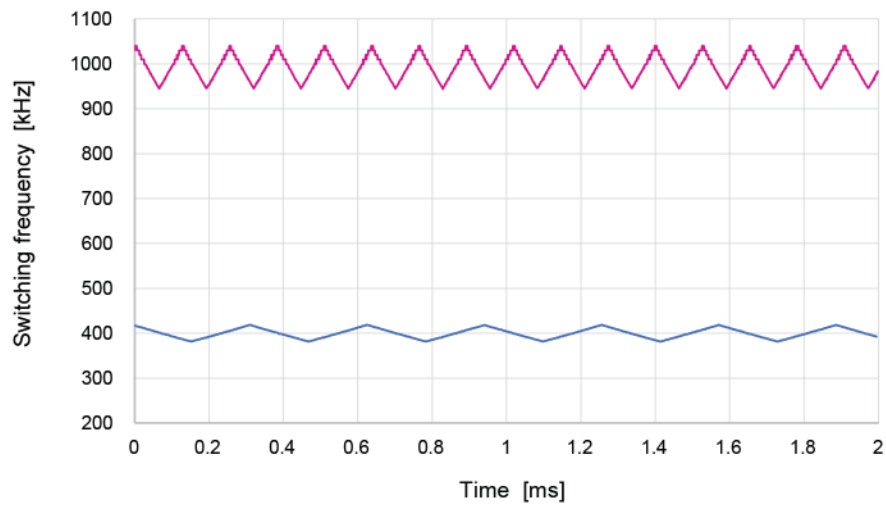
- Ramps up in 63 steps from minimum to maximum FSW
- Ramps down in 63 steps from maximum to minimum FSW

The modulation shape is almost triangular with a frequency of:

$$F_{Dithering} = \frac{F_{SW}}{126} \quad (2)$$

A visual explanation about how the switching frequency varies when the spread spectrum feature is used can be observed in Figure 13.

Figure 13. Switching frequency trend with spread spectrum feature activated



5.2 Transformer

The transformer is the key component for the iso-buck, ensuring the desired isolation as well as allowing the energy transfer to the secondary side, hence generating the secondary isolated output voltage.

More details about the transformer selection are provided in the dedicated section (see [Section 10.2 Transformer selection](#)).

5.3 Secondary side

The secondary side includes an LC filter (secondary winding of the transformer and secondary output capacitor) and the rectifying element (Schottky diode).

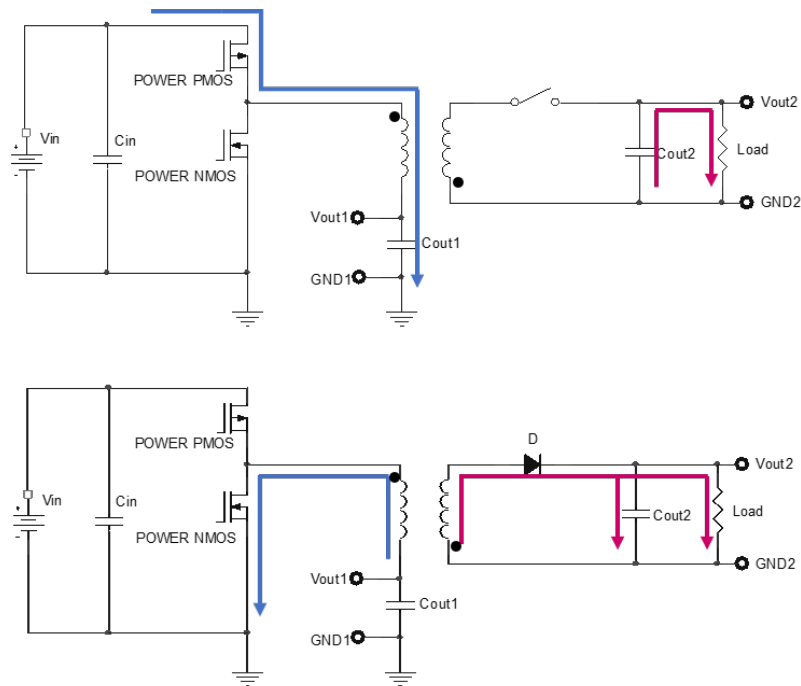
5.4 Iso-buck operation principle

The picture below describes the operation principle of the iso-buck converter.

When the high-side MOSFET is turned on, the current flows through the primary winding of the transformer and charges the primary output capacitor. Considering the dot convention of the transformer, the voltage at the anode of the Schottky diode is negative, hence the diode is reverse biased and no current flows in the secondary winding. The load connected to the secondary output is supplied by C_{OUT2} .

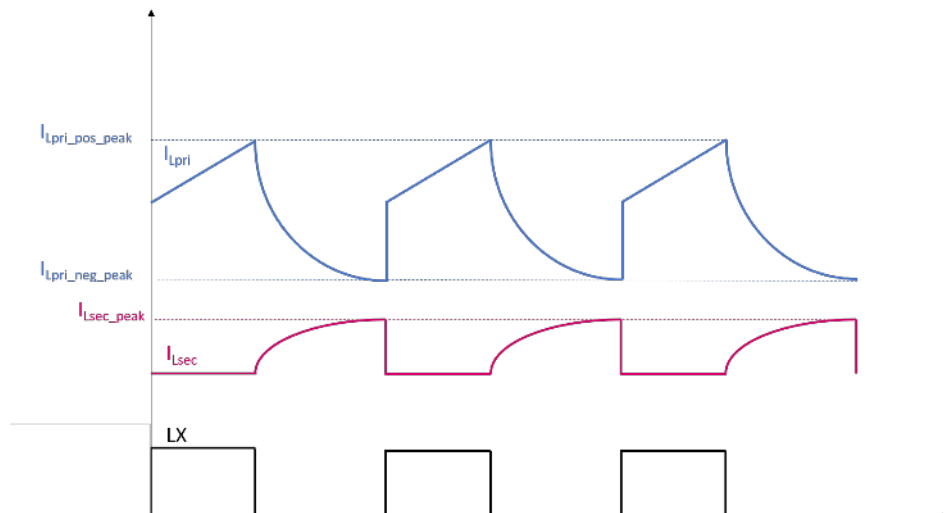
When the low-side MOSFET is turned on, the voltage applied at the transformer windings inverts its polarity. As consequence, the Schottky diode is now forward biased and allows the current to flow from the secondary winding to C_{OUT} and the load. Under this condition the energy transfer from primary to secondary side occurs.

Figure 14. Iso-buck basic operating principle



The waveforms in the figure below reproduce the trend of the current in the two windings in according to the switch node transitions.

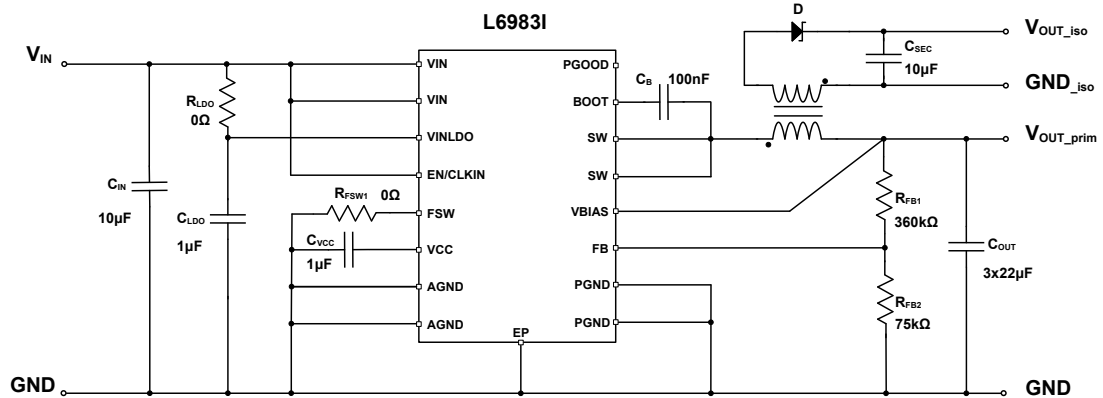
Figure 15. Iso-buck primary and secondary current waveforms



6 Iso-buck performances

All results shown in this section come from measurements performed using the reference schematic depicted in Figure 16.

Figure 16. Reference schematic for measurements of line and load regulation and efficiency

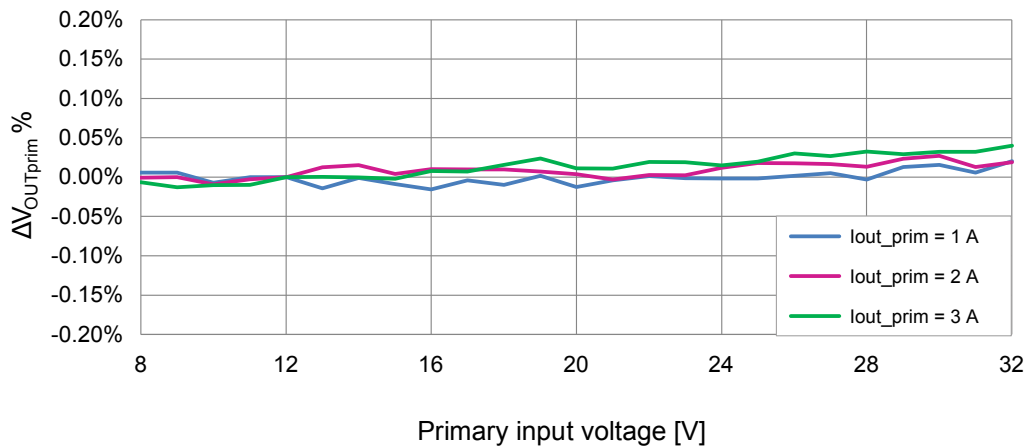


6.1 Output voltage line regulation

Primary output line regulation

The regulator features an enhanced primary line regulation due to the peak current mode architecture. Figure 17 shows the negligible output voltage variation (normalized to the value measured at $V_{IN} = 12\text{ V}$) over an input voltage range up to 32 V for L6983I with $V_{OUT_prim} = 5\text{ V}$, at three different output currents ($N = 6$).

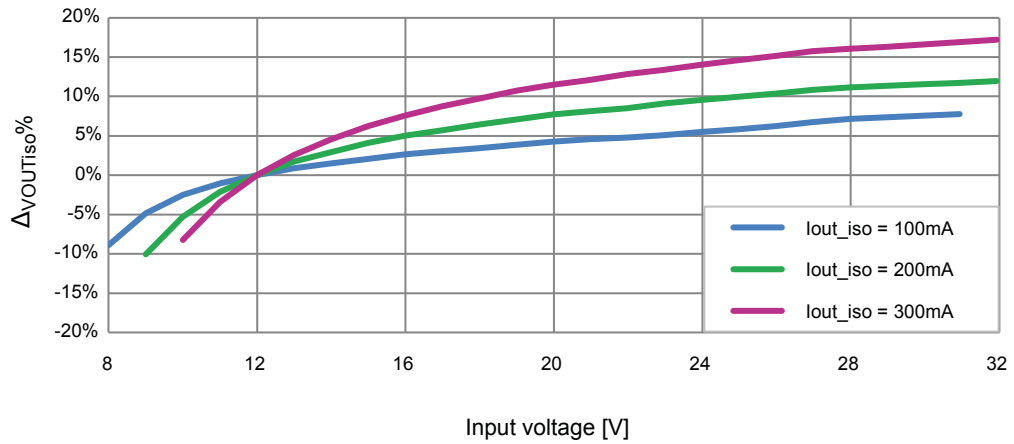
Figure 17. Primary output line regulation ($V_{OUT_prim} = 5\text{ V}$, $f_{SW} = 400\text{ kHz}$)



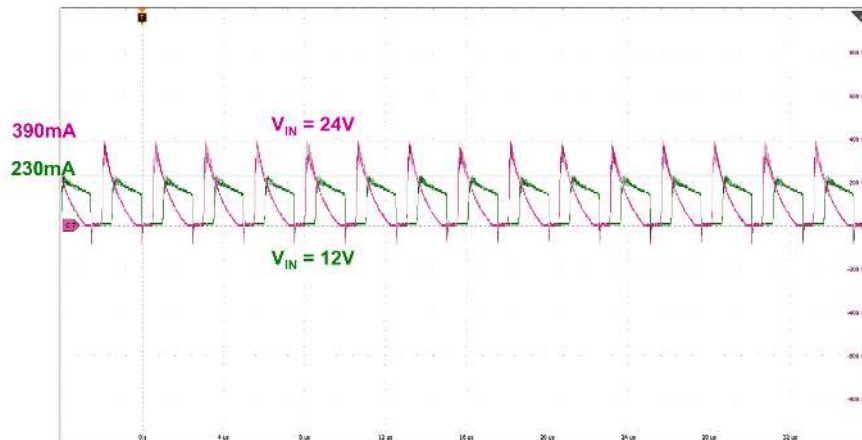
Secondary output line regulation

The secondary output line regulation is defined, similarly to the primary side, as the variation of secondary the output voltage due to the input voltage change at a specific current. The secondary output line regulation is mainly affected by the transformer and in particular by its leakage inductance.

Keeping constant the leakage inductance (that is, using the same transformer), a higher input voltage causes the isolated output voltage to slightly increase, as shown in Figure 18.

Figure 18. Secondary output line regulation ($V_{OUT_prim} = 5\text{ V}$, $f_{SW} = 400\text{ kHz}$, $N = 6$)


The input voltage value influences the peak current in the secondary winding (see [Figure 19](#)), hence determining the amount of energy delivered to the secondary output and in turn the isolated output voltage value.

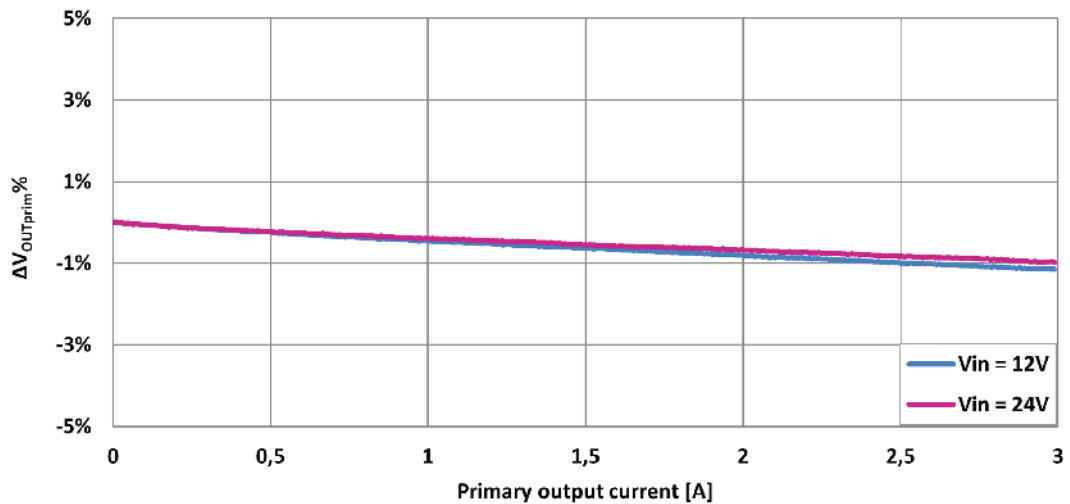
Figure 19. Secondary winding current at different input voltages


6.2 Output voltage load regulation

Primary output load regulation

Figure 20 shows negligible primary output voltage variation (normalized to the value measured at $I_{OUT} = 0$ A) over the entire output current range for the L6983I with $V_{OUT_{prim}} = 5$ V.

Figure 20. Load regulation of the primary not isolated output voltage ($V_{IN} = 12$ V, $V_{OUT_{prim}} = 5$ V, $f_{SW} = 400$ kHz)

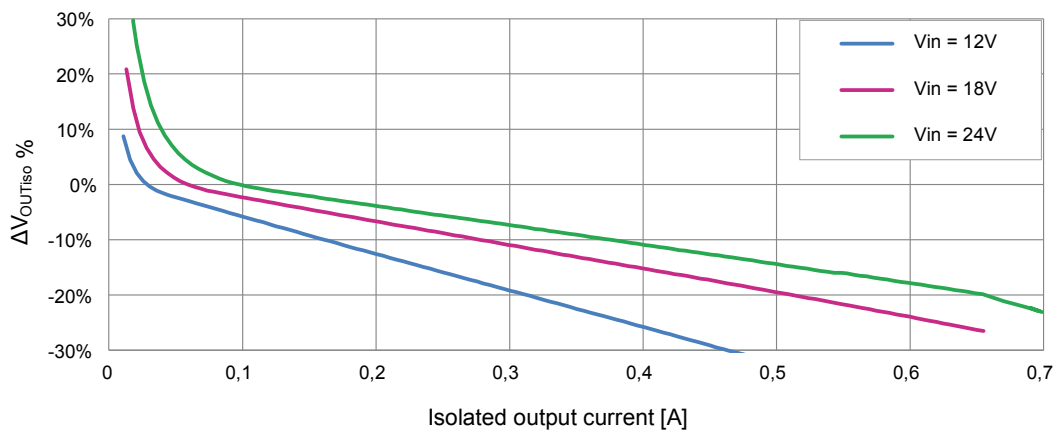


Secondary output load regulation

Since there is no regulation loop involving the secondary output, its load regulation depends, to some extent, on the primary load regulation and is affected by the leakage inductance (see Figure 22) of the transformer, the voltage drops across to the Schottky diode (diode forward voltage) and the DCR of the secondary coil, as indicated by the equation (Eq. (1)) (where only the last two contributions are considered). Minimizing all the mentioned parameters leads to a better load regulation.

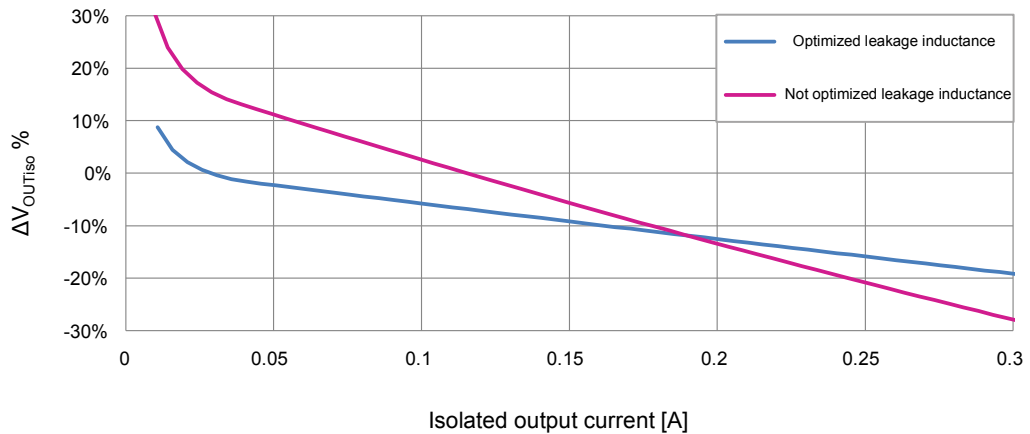
As shown in Section 6.1, the input voltage also plays a role in the isolated output regulation, as depicted by Figure 21.

Figure 21. Load regulation of the secondary isolated output voltage ($V_{IN} = 12$ V, $V_{OUT_{prim}} = 5$ V, $f_{SW} = 400$ kHz, $N = 6$)



The dependency of the isolated output voltage on the leakage is demonstrated by Figure 22, where the load regulations with two different transformers are compared. The optimized solution implements the same inductor of the demoboard described in section Section 11 , (ZB1346-AE, whose leakage inductance is around 1% of the magnetizing inductance, as typically recommended). The not optimized solution consists of the use of a transformer with a higher leakage inductance (twice as much the other transformer).

Figure 22. Effect of the transformer leakage inductance on the isolated output load regulation ($V_{IN} = 12\text{ V}$, $V_{OUT_prim} = 5\text{ V}$, $N = 6$)



6.3 Efficiency

Primary output

Figure 23 shows the efficiency referred to the primary output, at two different input voltages, achieving a peak value of almost 90%.

Figure 23. Primary output efficiency ($V_{OUT_prim} = 5\text{ V}$, $f_{SW} = 400\text{ kHz}$, secondary isolated output not loaded)

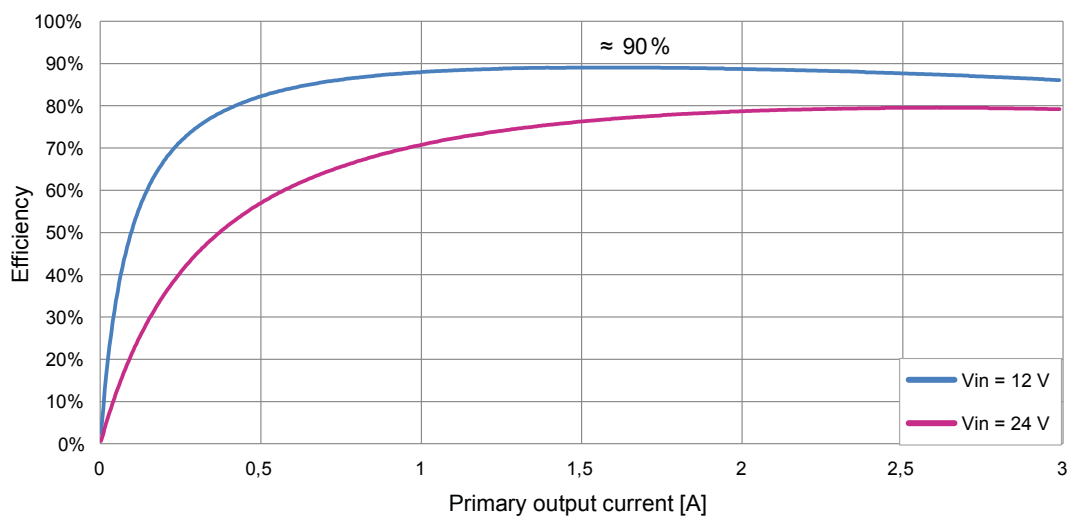
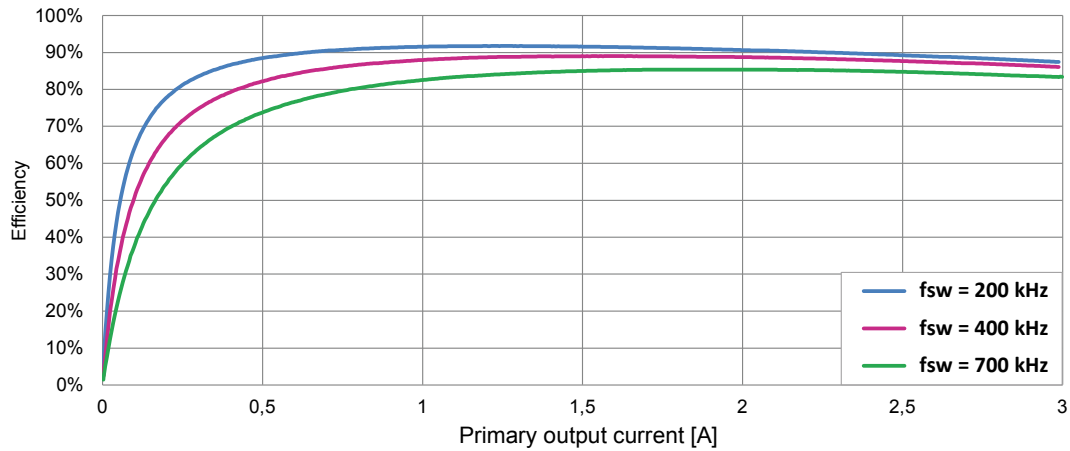


Figure 24 compares instead the efficiency trends depending on the switching frequency, whose effect dominates at lower currents.

Figure 24. Primary output efficiency vs. switching frequency ($V_{IN} = 12\text{ V}$, $V_{OUT_prim} = 5\text{ V}$, secondary isolated output (not loaded))



Secondary isolated output

Figure 25 shows the efficiency referred to the secondary isolated output at different input voltages, whose effect on the efficiency is more evident at lower currents.

Figure 25. Secondary isolated output efficiency at different input voltages ($V_{OUT_prim} = 5\text{ V}$, $f_{SW} = 400\text{ kHz}$, $N = 6$)

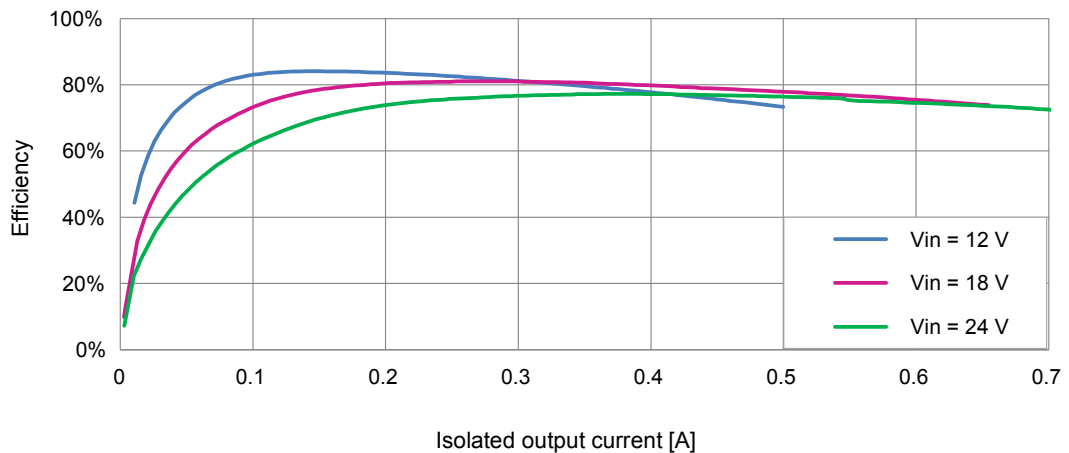
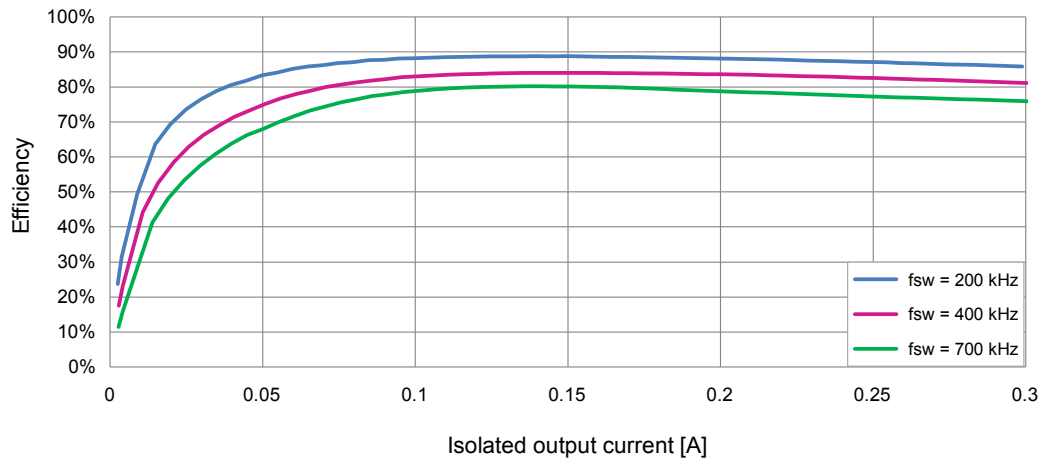


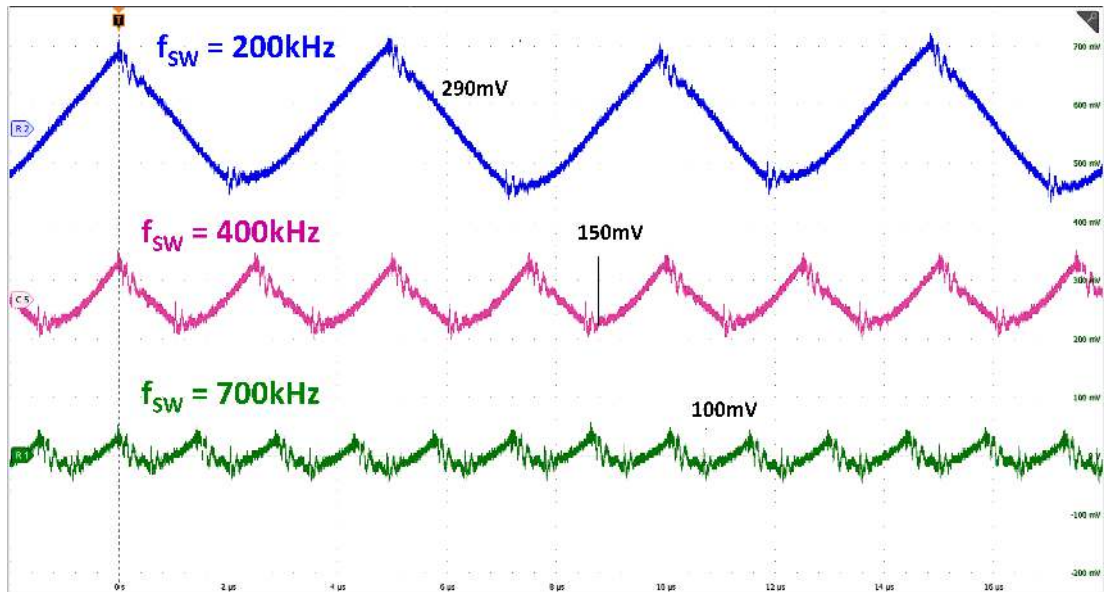
Figure 26 depicts the efficiency variation with the switching frequency. A lower switching frequency contributes to a better efficiency by improving the load regulation (higher isolated output voltage, that is, higher power), in addition to the obvious lower switching losses.

Figure 26. Secondary output efficiency vs. switching frequency ($V_{IN} = 12\text{ V}$, $V_{OUT_prim} = 5\text{ V}$, $N = 6$)



Selecting a lower switching frequency impacts however on the transformer size and on the ripple (see Figure 27) requiring therefore a higher output capacitance to reduce it.

Figure 27. Isolated output voltage ripple vs. switching frequency ($C_{OUTiso} = 10\text{ }\mu\text{F}$)



7 Device protections

7.1 Overvoltage protection

The overvoltage is a second level protection, and it should never be triggered in normal operating conditions if the system is properly dimensioned. In other words, the selection of the external power components and the dynamic performance determined by the compensation network should guarantee an output voltage regulation within the overvoltage threshold even during the worst-case scenario in terms of load transitions.

7.2 Overcurrent protection

Primary side

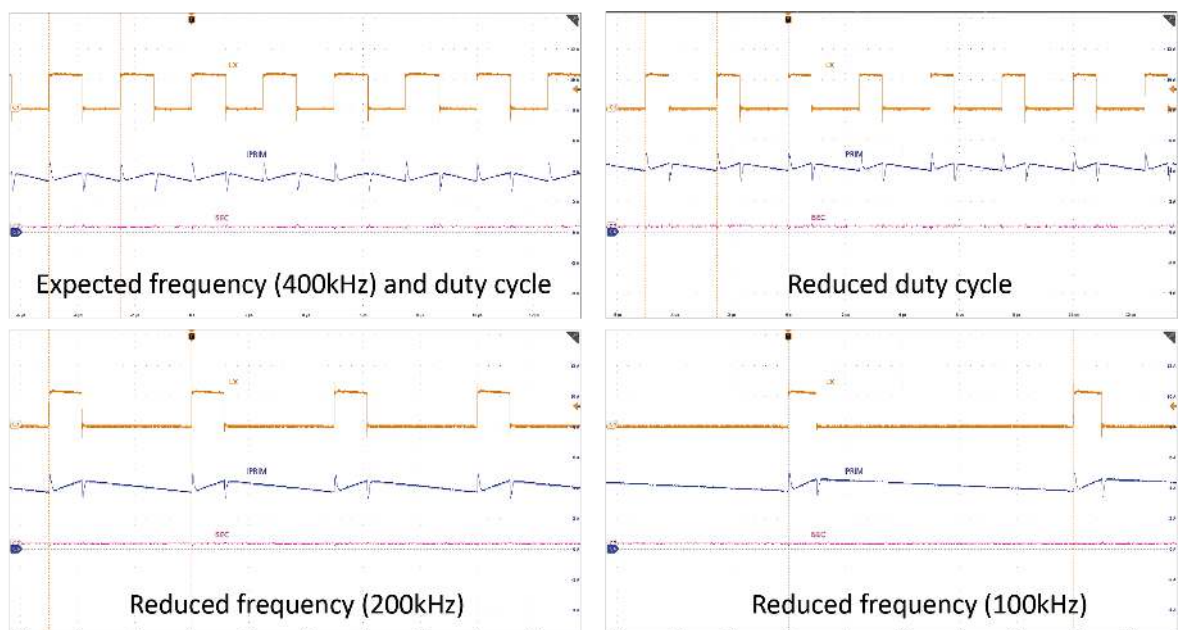
The current protection circuitry features a constant current protection, so the device limits the maximum peak current (see Table 6. Electrical characteristics) in an overcurrent condition.

The L6983I device implements a pulse-by-pulse current sensing on both power elements (high-side and low-side switches) for effective current protection over the duty cycle range. The high-side current sensing is called “peak”, the low-side sensing “valley”.

The internal noise generated during the switching activity makes the current sensing circuitry ineffective for a minimum conduction time of the power element. This time is called “masking time” (see section Section 5.1.4 Minimum on-time) because the information from the analog circuitry is masked by the logic to prevent an erroneous detection of the overcurrent event. Therefore, the peak current protection is disabled for a masking time (typ. 390 ns) after the high-side switch is turned on. The masking time for the valley sensing (T_{OFF_MIN} , see Table 6. Electrical characteristics) is activated after the low-side switch is turned on. In other words, the peak current protection can be ineffective at extremely low duty cycles, the valley current protection at extremely high duty cycles.

The L6983I device assures an effective overcurrent protection sensing the current flowing in both power elements. In case one of the two current sensing circuitries is ineffective because of the masking time, the device is protected sensing the current on the opposite switch. Thus, the combination of the “peak” and “valley” current limits (I_{PK} and I_{VY} respectively) assure the effectiveness of the overcurrent protection even in extreme duty cycle conditions.

Figure 28. Effects of the peak and valley current protections on duty cycle and frequency



The current limit intervention might affect the duty cycle as well as the frequency. Reaching the peak current limit implies a duty cycle reduction (until the T_{ON_MIN} is reached). When the low-side switch is on, as long as the current is above the I_{VY} , any new clock cycle is ignored. The switching frequency is hence reduced. These effects of both duty cycle and switching frequency are summarized in Figure 28.

A short-circuit at the primary output is a particular case of overcurrent. Figure 29 shows the behavior of the device in case of a short-circuit present before the soft-start.

Figure 29. Soft-start procedure with short-circuit at the primary output

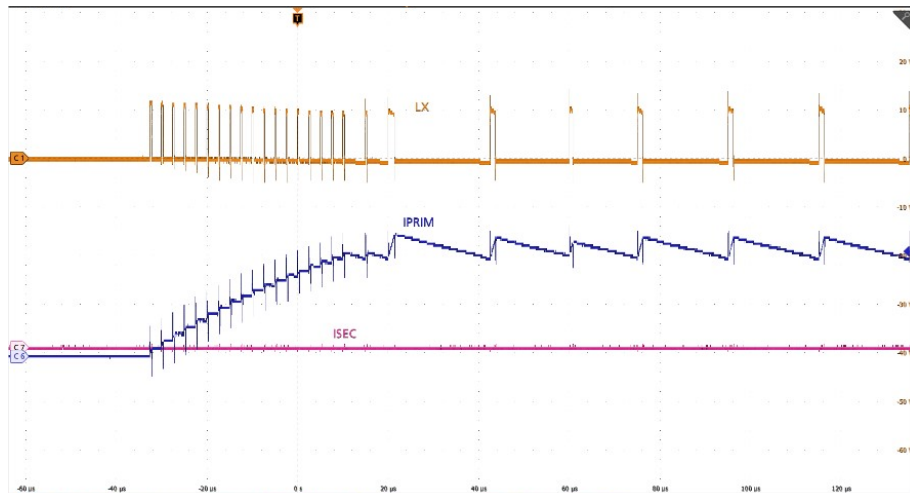
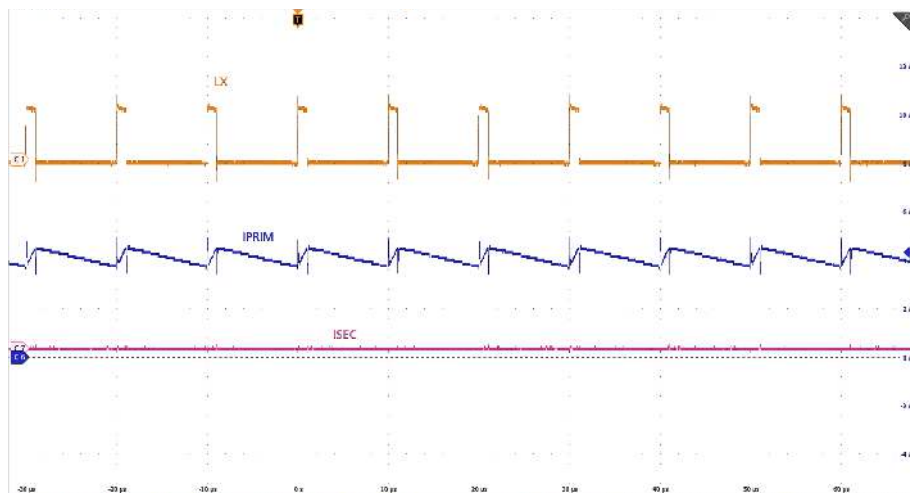


Figure 30 shows a persistent short-circuit condition (frequency reduced from 400 kHz to 100 kHz).

Figure 30. Overcurrent procedure in case of persistent short-circuit at the primary output



Secondary side

The increase of the secondary output current affects the current shape at primary side. In particular, the peak currents in the high-side and low-side MOSFETs rise (in absolute value in the low-side, that is, the current becomes more negative), in accordance with equations (Eq. (3)) and (Eq. (4)).

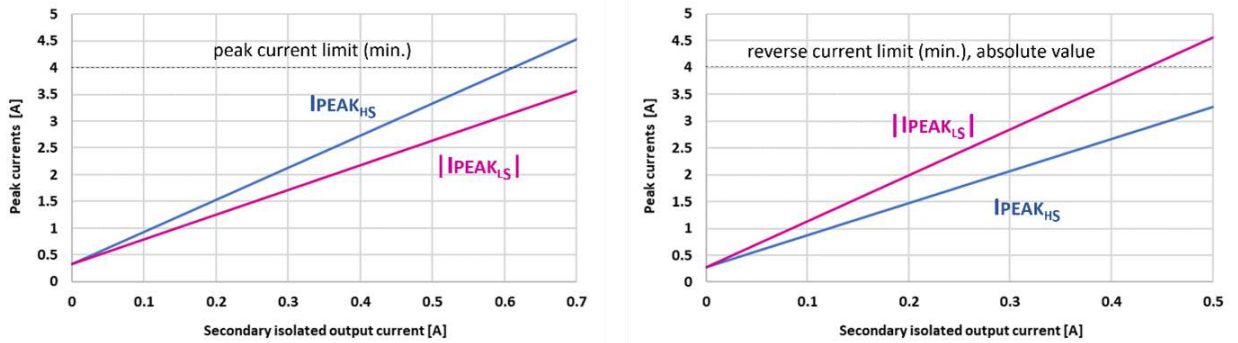
$$I_{PEAK_{HS}} = I_{OUT_pri} + N \cdot I_{OUT_sec} + \frac{\Delta I_L}{2} \quad (3)$$

$$I_{PEAK_{LS}} = -N \cdot I_{OUT_sec} \cdot \left(\frac{2D}{1-D} \right) - \frac{\Delta I_L}{2} + I_{OUT_prim} \quad (4)$$

where I_{OUT_pri} and I_{OUT_sec} are respectively the primary and secondary output currents, N is the transformer turn ratio, D the duty cycle and ΔI_L the current ripple in the primary winding.

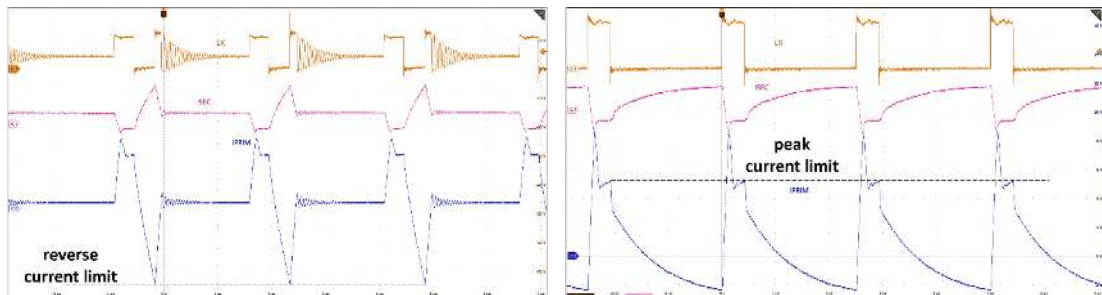
Figure 31 depicts how these peak currents vary depending on the secondary output current, under the specified conditions.

Figure 31. Peak currents in LS and HS MOSFET depending on the isolated output current ($V_{IN} = 12\text{ V}$, $V_{OUT_prim} = 5\text{ V}$, $N = 6$)



Depending on the application conditions (for example, duty cycle and therefore the input voltage), the peak or the reverse current limit can be first exceeded and hence represents the limitation of the secondary isolated output current (see Figure 32).

Figure 32. Left: $V_{IN} = 12\text{ V}$, I_{PRIM} exceeds I_{V_SINK} . Right: $V_{IN} = 18\text{ V}$, I_{PRIM} exceeds I_{PK} .



Once the reverse current limit is crossed, the device turns the LS MOSFET off and the current flows in the body diode of the HS MOSFET until it reaches zero. Both HS and LS MOSFET remain off until the next clock cycle.

7.3 Thermal shutdown

The shutdown block disables the switching activity if the junction temperature is higher than a fixed internal threshold (T_{SHDOWN} refer to Table 6. Electrical characteristics). The thermal sensing element is close to the power elements, ensuring fast and accurate temperature detection. A hysteresis of approximately $30\text{ }^{\circ}\text{C}$ prevents the device from turning ON and OFF too fast. After a thermal protection event has expired, the L69831 restarts with a new soft-start.

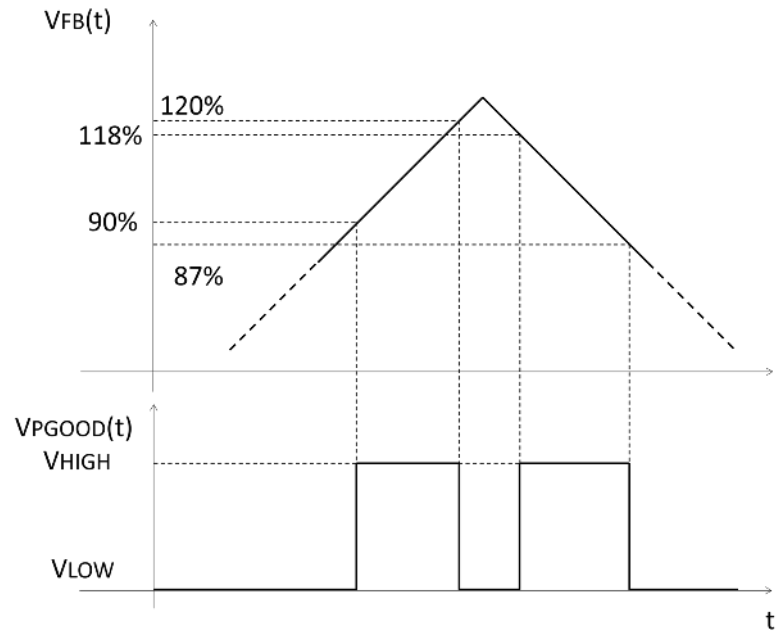
7.4 Power good

The PGOOD pin indicates whether the output voltage is within its regulation level. The pin output is an open drain MOSFET. The PG is pulled low:

1. When the FB pin voltage is lower than 90 % (typ.) of the nominal internal reference for more than $10\text{ }\mu\text{s}$.
2. When the FB pin voltage is higher than 120% (typ.) of the nominal internal reference for more than $10\text{ }\mu\text{s}$.
3. During the soft-start procedure also with pre-charged V_{OUT} .
4. If a thermal shutdown event occurs.
5. If a UVLO event occurs.

The PGOOD pin is V_{IN} compatible.

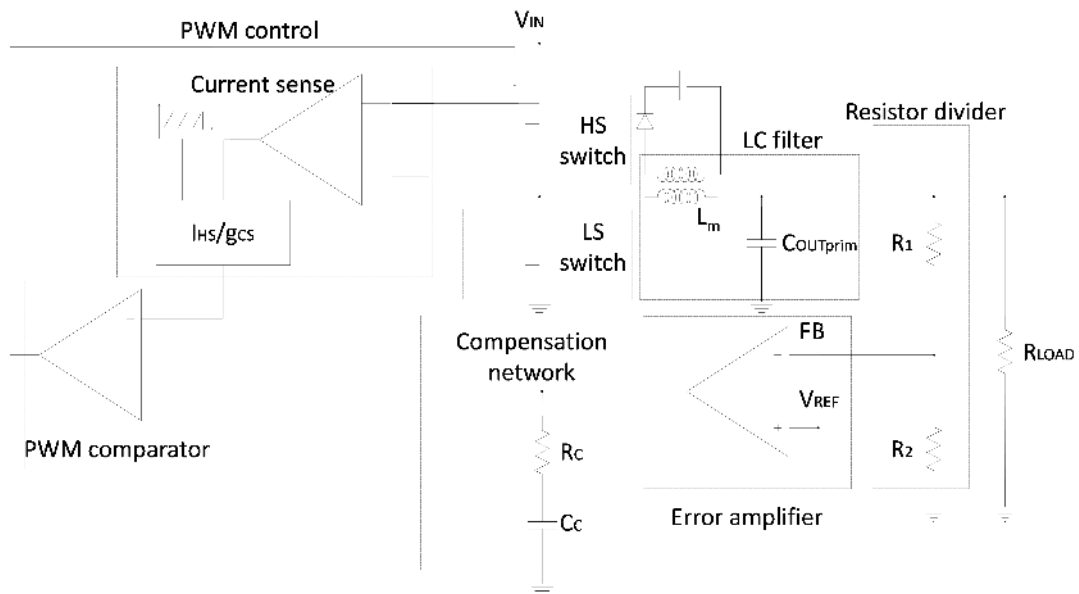
Figure 33. PGOOD thresholds



8 Closing the loop

The iso-buck, compared to a standard buck, includes the transformer in place of the inductor and all the components connected to the secondary winding (at least the Schottky diode and the secondary output capacitor). Nevertheless, the regulation loop does not include the secondary side components. As a first approximation the control loop of an iso-buck can be assimilated to the one of a standard buck. Therefore, the block diagram in the figure below can still be used (where the inductor symbol identifies the inductance of the primary winding) as well as all the equations and calculations in the next sections.

Figure 34. Block diagram of the loop



8.1 $G_{CO}(s)$ control to output transfer function

The accurate control to output transfer function for a buck peak current mode converter can be written as:

$$G_{CO}(s) = R_{LOAD} \cdot g_{CS} \cdot \frac{1}{1 + \frac{R_{LOAD} \cdot T_{SW}}{L} \cdot [m_C \cdot (1-D) - 0.5]} \cdot \frac{1 + \frac{s}{\omega_Z}}{1 + \frac{s}{\omega_P}} \cdot F_H(s) \quad (5)$$

where R_{LOAD} represents the load resistance, g_{CS} the equivalent sensing transconductance of the current sense circuitry, ω_P the single pole introduced by the power stage and ω_Z the zero given by the ESR of the output capacitor.

$F_H(s)$ accounts the sampling effect performed by the PWM comparator on the output of the error amplifier that introduces a double pole at one half of the switching frequency.

$$\omega_Z = \frac{1}{ESR \cdot C_{OUT}} \quad (6)$$

$$\omega_P = \frac{1}{R_{LOAD} \cdot C_{OUT}} \cdot \frac{m_C \cdot (1-D) - 0.5}{L \cdot C_{OUT} \cdot f_{SW}} \quad (7)$$

where:

$$\left\{ \begin{array}{l} m_C = 1 + \frac{S_e}{S_n} \\ S_e = V_{PP} \cdot g_{CS} \cdot f_{SW} \\ S_n = \frac{V_{IN} - V_{OUT}}{L} \end{array} \right. \quad (8)$$

Where I_{SLOPE} is equal to 1 [A].

S_n represents the on-time slope of the sensed inductor current, S_e the on-time slope of the external ramp that implements the slope compensation to avoid sub-harmonic oscillations at duty cycle over 50%.

The sampling effect contribution $F_H(s)$ is:

$$F_H(s) = \frac{1}{1 + \frac{s}{\omega_n \cdot Q_p} + \frac{s^2}{\omega_n^2}} \quad (9)$$

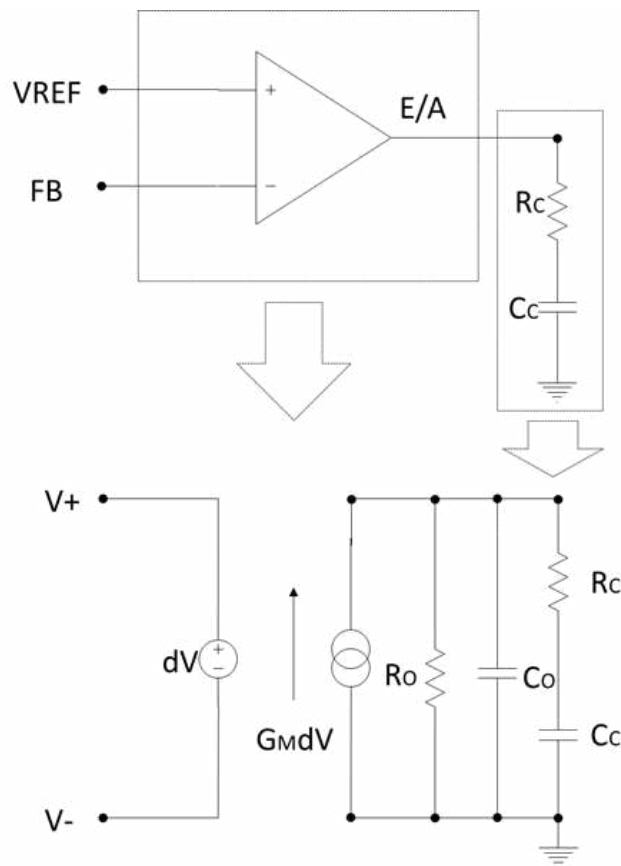
where

$$Q_p = \frac{1}{\pi \cdot [m_C \cdot (1 - D) - 0.5]} \quad (10)$$

8.2 Error amplifier compensation network

The following figure shows the typical compensation network required to stabilize the system.

Figure 35. Transconductance embedded error amplifier



R_C and C_C introduce a pole and a zero in the open loop gain. The transfer function of the error amplifier and its compensation network is:

$$A_O(s) = \frac{A_{VO} \cdot (1 + s \cdot R_C \cdot C_C)}{s^2 \cdot R_O \cdot C_O \cdot R_C \cdot C_C + s \cdot (R_O \cdot C_C + R_O \cdot C_O + R_C \cdot C_C) + 1} \quad (11)$$

where:

$$A_{VO} = G_m \cdot R_O \quad (12)$$

The poles of this transfer function are (if $C_C \gg C_O$):

$$f_{PLF} = \frac{1}{2 \cdot \pi \cdot R_O \cdot C_C} \quad (13)$$

$$f_{PHF} = \frac{1}{2 \cdot \pi \cdot R_O \cdot C_O} \quad (14)$$

Whereas the zero is defined as:

$$f_Z = \frac{1}{2 \cdot \pi \cdot R_C \cdot C_C} \quad (15)$$

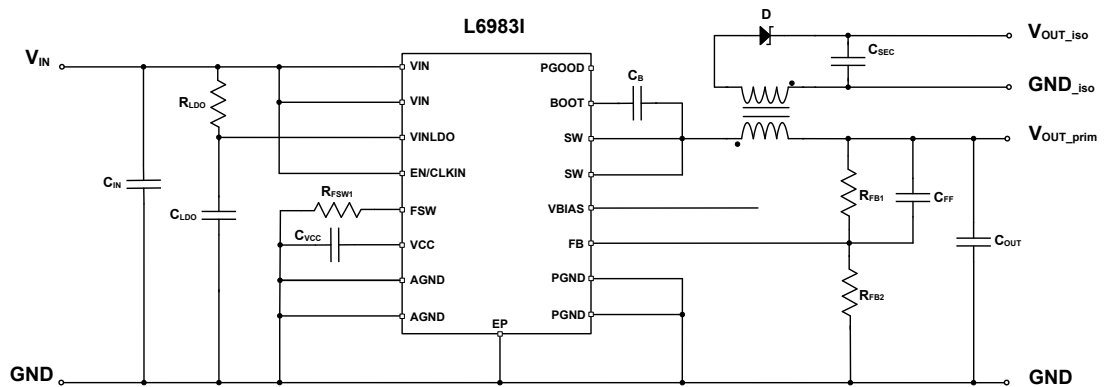
8.3 Voltage divider

The contribution of a simple voltage divider is:

$$G_{DIV}(s) = \frac{R_2}{R_1 + R_2} \quad (16)$$

A small signal capacitor in parallel to the upper resistor (only for the adjustable part number) of the voltage divider implements a leading network ($f_{ZERO} < f_{POLE}$), sometimes necessary to improve the system phase margin:

Figure 36. Contribution of the resistor divider



Laplace transformer of the leading network:

$$G_{DIV}(s) = \frac{R_2}{R_1 + R_2} \cdot \left(\left(1 + s \cdot R_1 \cdot C_{R1} \right) / \left(\left(1 + s \cdot \frac{R_1 \cdot R_2}{R_1 + R_2} \right) \cdot C_{R1} \right) \right) \quad (17)$$

where:

$$f_z = \frac{1}{2 \cdot \pi \cdot R_1 \cdot C_{R1}} \quad (18)$$

$$f_P = \frac{1}{2 \cdot \pi \cdot \frac{R_1 \cdot R_2}{R_1 + R_2} \cdot C_{R1}} \quad (19)$$

$$f_z < f_P \quad (20)$$

So closing the loop, the loop gain is:

$$G(s) = G_{DIV}(s) \cdot G_{CO}(s) \cdot A_O(s) \quad (21)$$

9 Application notes

9.1 Output voltage adjustment

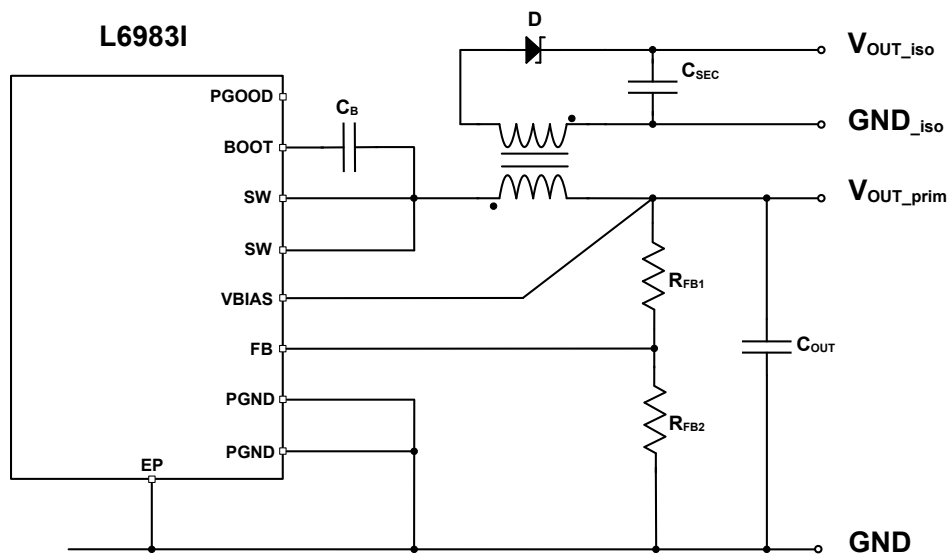
Primary output voltage

The error amplifier reference voltage is 0.85 V typical. The output voltage is adjusted according to the equation below:

$$V_{OUT_prim} = 0.85 \cdot \left(1 + \frac{R_{FB1}}{R_{FB2}} \right) \quad (22)$$

where R_{FB1} and R_{FB2} are the resistors used in the output divider (see figure below).

Figure 37. Primary output voltage regulation



A general recommendation is to keep the duty cycle below 50-60%. A higher duty cycle would limit off-time, limiting the time in which the energy transfer to the secondary side takes place.

Other restrictions in the duty cycle selection arise due to the minimum on-time (see Section 9.2 Switching frequency), generally summarized by the following equation:

$$D \geq D_{MIN} = T_{ON_MIN} \cdot f_{SW} \quad (23)$$

Secondary output voltage

In the iso-buck converter, the secondary output voltage is not included in the regulation loop. Nevertheless, a good regulation of the secondary output voltage is achieved by relying on the primary output voltage regulation, and the selection of a proper turn ratio of the transformer as well as considering the voltage drops due to the secondary winding resistance and the Schottky diode. That can be summarized by the following equation:

$$V_{OUT_sec} = N \cdot \left[V_{OUT_prim} + I_{OUT_pri} \cdot (R_{DS(on)} + R_{wind_pri}) \right] \cdot \frac{L_m}{L_m + L_{LEAK}} - R_{wind_sec} \cdot I_{OUT_sec} - V_{FD1} \quad (24)$$

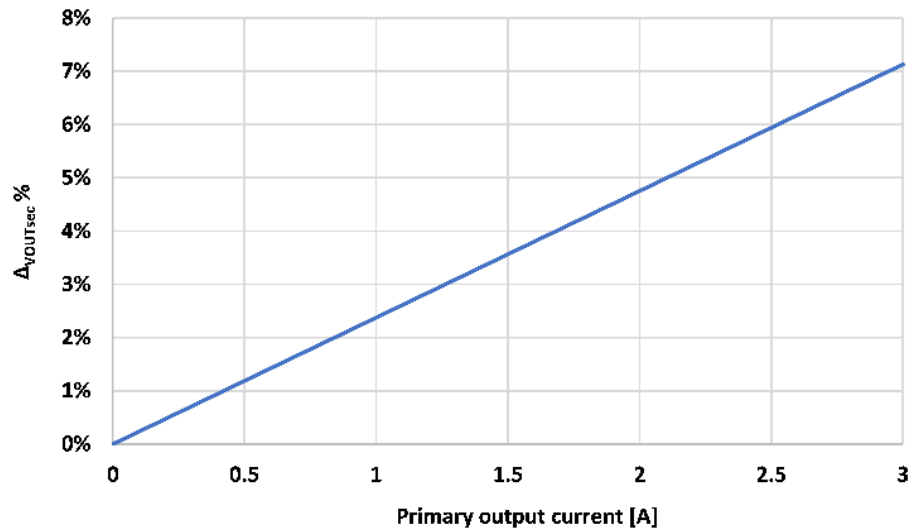
Where N is the turn ratio, R_{wind_prim} and R_{wind_sec} are the winding resistances of the primary and secondary side respectively, V_{FD1} is the forward voltage of the Schottky diode, L_m is the magnetizing inductance of the transformer and L_{LEAK} the leakage inductance of the transformer.

If no current is drawn from the primary output, equation 24 can be simplified as follows:

$$V_{OUT_sec} = N \cdot V_{OUT_prim} \cdot \frac{L_m}{L_m + L_{LEAK}} - R_{wind_sec} \cdot I_{OUT_sec} - V_{FD1} \quad (25)$$

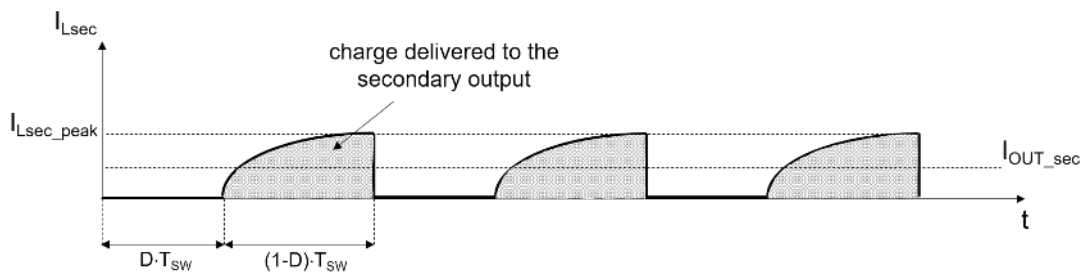
Eq. (25) emphasizes how the selection of the transformer and, to some extent, the Schottky diode play a crucial role in the accurate regulation of the secondary output voltage. Figure 38 shows instead the effect of the current drawn from the primary output on the isolated voltage, as described by the Eq. (24).

Figure 38. Isolated voltage variation due to the primary output current



Another factor affecting the secondary output voltage regulation comes from the leakage inductance of the transformer. As described later on, the leakage inductance determines the peak current that can be reached in the secondary winding. This peak current defines the maximum current from the secondary isolated output by limiting the amount of charge delivered to the output. When the current demand from the secondary isolated output exceeds the maximum deliverable charge limited by the peak current, the isolated output voltage drops.

Figure 39. Secondary output maximum current



The effect of the leakage on the load regulation was already shown in Figure 22 in Section 6.2 .

To some extent also the duty cycle can affect the secondary output voltage. Since the energy transfer from primary to secondary occurs only during the T_{OFF} , a too high duty cycle could reduce the achievable peak current, hence limiting the deliverable current to the secondary output. Under this condition, the secondary output could drop.

9.2 Switching frequency

A resistor connected to the FSW pin features the selection of the switching frequency (refer to Section 4.1 Frequency selection table).

Connecting the resistor between the pins F_{SW} and V_{CC} , the internal dithering circuit is turned on (see Figure 3).

The selection of the switching frequency must take into account the minimum on-time of the device ($T_{ON MIN}$, as indicated in the electrical characteristics table), as described by the following equation:

$$f_{SW_max} \leq \frac{V_{OUT}}{T_{ON MIN} \cdot V_{IN} \cdot \eta} \quad (26)$$

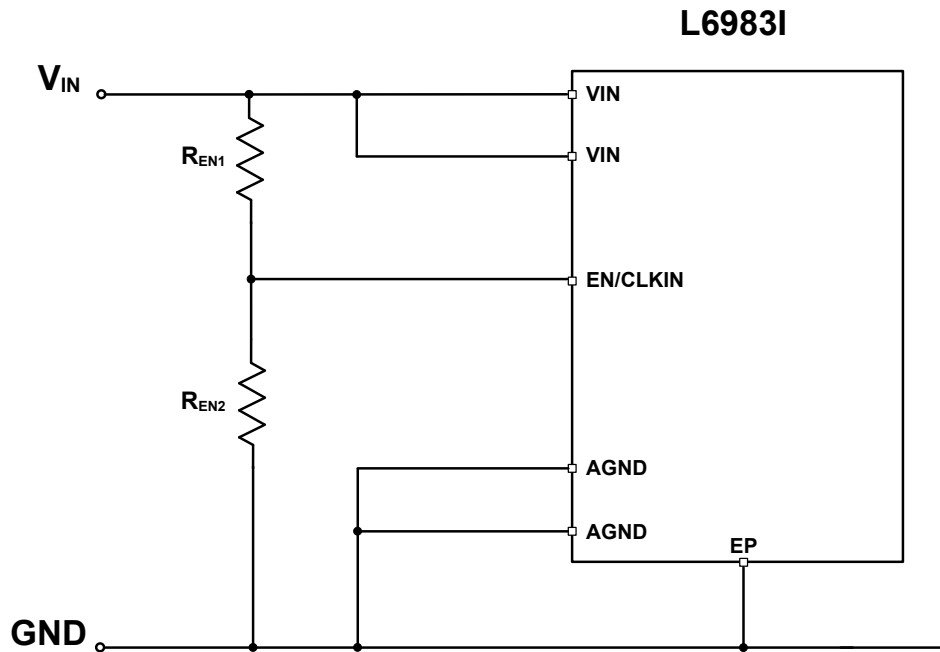
The switching frequency affects the selection of the primary inductance as well as the transformer construction. The efficiency also varies with the switching frequency (see Figure 24 and Figure 26).

9.3 Programmable power-up threshold

The Enable rising threshold is equal to 1.2 V typical (refer to Table 6. Electrical characteristics). The power-up threshold is adjusted according to the following equation:

$$V_{Power UP} = 1.2 \cdot \left(1 + \frac{R_{EN1}}{R_{EN2}}\right) \quad (27)$$

Figure 40. Programming power-up threshold



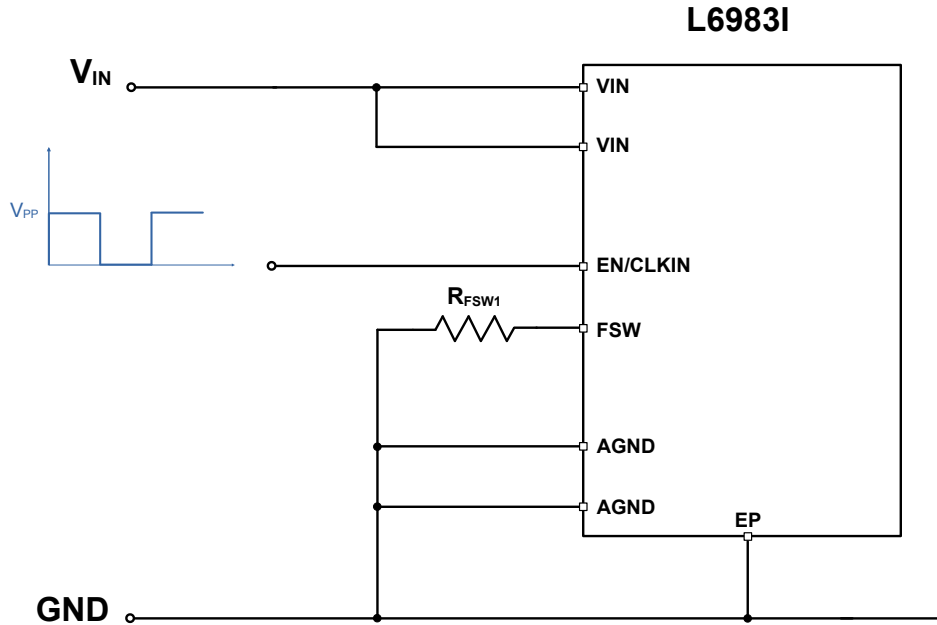
The Enable falling threshold is equal to 1.0 V typical (refer to Table 6. Electrical characteristics). The turn threshold is obtained according to the following equation:

$$V_{Power Down} = 1.0 \cdot \left(1 + \frac{R_{EN1}}{R_{EN2}}\right) \quad (28)$$

9.4 Output External synchronization

The device allows a direct connection between a clock source and the EN/CLKIN pin.

Figure 41. External synchronization (direct connection)



The device internally implements a low-pass filter connected to the EN/CLKIN pin that is able to acquire the average value of the applied signal.

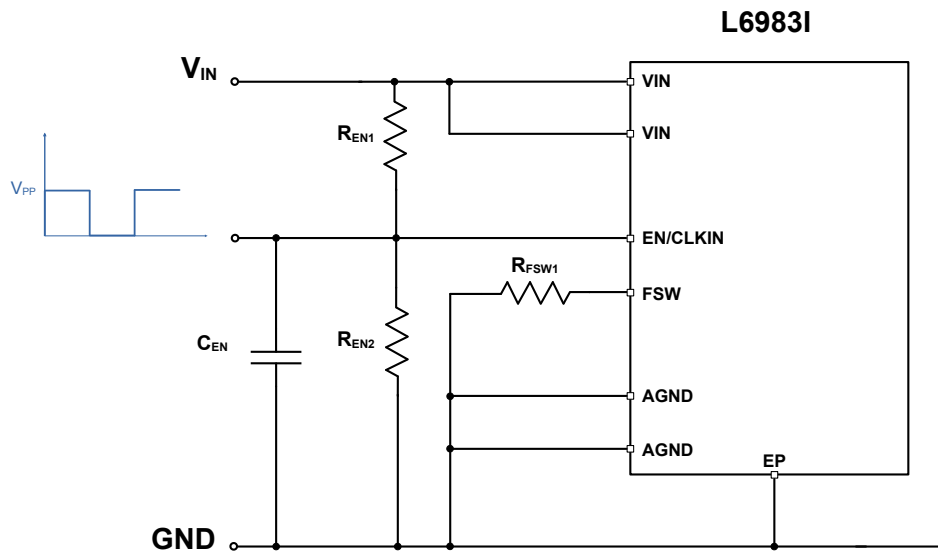
The device turns on when the average of the signal applied is higher than V_{EN} rising (refer to [Table 6. Electrical characteristics](#)). The device turns off when the average of the signal should be lower than V_{EN} falling (refer to [Table 6. Electrical characteristics](#)). Considering, for example, a clock source with $V_{PP} = 5.0$ V, the minimum duty cycle to guarantee the power-up is given by:

$$\text{Duty}_{\min} = \frac{V_{EN, \text{Rising}}}{V_{PP}} = 0.24 \quad (29)$$

The maximum duty cycle to guarantee the turn-off is given by:

$$\text{Duty}_{\text{MAX}} = \frac{V_{EN, \text{Falling}}}{V_{PP}} = 0.2 \quad (30)$$

The device also allows the AC coupling.

Figure 42. External synchronization (AC coupling)


The AC-coupling allows the device to keep the power-up and down thresholds defined by the partition connected to the EN/CLKIN pin and described in [Section 9.3 Programmable power-up threshold](#).

The following table shows the minimum pulse duration for the external signal and maximum duty cycle that allows the synchronization by keeping the selected power-up and down thresholds.

Table 8. External synchronization AC coupling suggested operation range

V_{PP} [V]	T_{ON,MIN, EXT_Clock} [ns]	D_{MAX, EXT_Clock} [%]
2.3	60	45
3.3	20	30
5	20	20

The minimum amplitude for the external clock signal is, for both the configurations, equal to 2.3 V.

The network given by C_{EN} and R_{ENL} sets a high-pass filter. Considering a resistor in the order of 220 K Ω , a capacitor equal to 1 nF is a correct choice.

10 Design of the external components

10.1 Input capacitor selection

The input capacitor, just like in a standard buck, should limit the input voltage ripple. Key parameters of the input capacitor are, together with its value, the maximum operating voltage and the RMS current capability.

The input capacitor voltage rating must be higher than the maximum input operating voltage of the application. During the switching activity a pulsed current flows into the input capacitor and so its RMS current capability must be selected according to the application conditions. Internal losses of the input filter depend on the ESR value so usually low ESR capacitors (like multilayer ceramic capacitors) have higher RMS current capability. On the other hand, given the RMS current value, a lower ESR input filter has lower losses and so contributes to higher conversion efficiency.

The maximum RMS input current flowing through the capacitor can be calculated as:

$$I_{RMS} = \left(I_{OUT_pri} + \frac{I_{OUT_sec}}{N} \right) \cdot \sqrt{\left(1 - \frac{D}{\eta} \right) \cdot \frac{D}{\eta}} \quad (31)$$

In the ideal case of efficiency $\eta = 1$, the RMS current reaches its maximum value when $D = 0.5$.

In general, the maximum and minimum duty cycles can be calculated as:

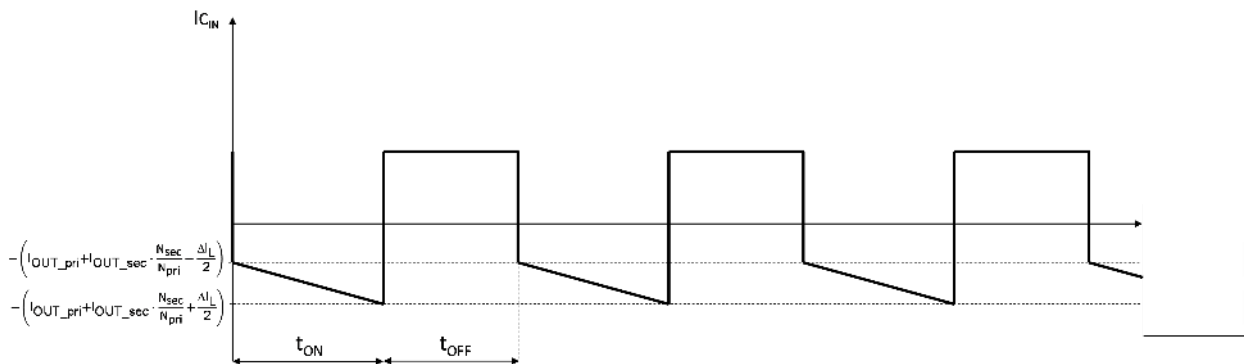
$$D_{MAX} = \frac{V_{OUT_pri} + \Delta V_{LS}}{V_{INmin} + \Delta V_{LS} - \Delta V_{HS}} \quad (32)$$

$$D_{MIN} = \frac{V_{OUT_pri} + \Delta V_{LS}}{V_{INmax} + \Delta V_{LS} - \Delta V_{HS}} \quad (33)$$

Where ΔV_{HS} and ΔV_{LS} are the voltage drop across the high-side and low-side MOSFETs respectively.

The AC component of the input current (see figure below) flows in the input capacitor, generating the input voltage ripple.

Figure 43. Input capacitor AC current



The peak to peak voltage across the input capacitor can be calculated as follows:

$$V_{PP} = \left(\frac{I_{OUT_pri} + I_{OUT_sec} \cdot \frac{N_{sec}}{N_{pri}}}{C_{IN} \cdot f_{SW}} \right) \cdot \frac{D}{\eta} \cdot \left(1 - \frac{D}{\eta} \right) + ESR \cdot \left(I_{OUT_pri} + I_{OUT_sec} + \frac{\Delta I_L}{2} \right) \quad (34)$$

In case of negligible ESR (for example, in the case of MLCC capacitors) Eq. (34) can be simplified. The value of the input capacitor can be so derived:

$$C_{IN} = \frac{I_{OUT_pri} + I_{OUT_sec} \cdot \frac{N_{sec}}{N_{pri}}}{V_{PP} \cdot f_{SW}} \cdot \frac{D}{\eta} \cdot \left(1 - \frac{D}{\eta} \right) \quad (35)$$

Considering the ideal case of $\eta = 1$, the equation above reaches its maximum value when $D = 0.5$. Therefore, the minimum input capacitance value can be defined as follows:

$$C_{IN} \geq C_{INmin} = \frac{I_{OUT_pri} + I_{OUT_sec} \cdot \frac{N_{sec}}{N_{pri}}}{4 \cdot V_{PP} \cdot f_{SW}} \quad (36)$$

Typically, C_{IN} is dimensioned to keep the maximum peak to peak voltage across the input filter in the order of 5% of V_{INmax} .

10.2 Transformer selection

The transformer has two essential tasks:

- Providing the isolation between the primary and secondary side in accordance with the application requirements
- Generating the necessary secondary output voltage from the regulated primary voltage with the most suitable turn ratio

The transformer selection implies the definition of the following parameters:

- Isolation voltage
- Turn ratio
- Primary inductance
- Peak and RMS currents
- Windings resistance
- Leakage inductance
- Parasitic capacitances

Isolation voltage

The isolation of the transformer in terms of voltage capability (1.5 kV, 4 kV, and so on) and type (functional basic, reinforced, etc.) is mainly driven by the application. Both parameters normally affect the size of the transformer as well as other electrical characteristics (for example, winding resistance, leakage inductance, etc.).

Turn ratio

Naming N_{pri} and N_{sec} the number of turns of the primary and secondary windings respectively, the turn ratio is so defined:

$$N = \frac{N_{sec}}{N_{prim}} \quad (37)$$

Considering Eq. (24), the turn ratio must be defined so that the voltage at the secondary output is the desired one over the whole secondary output current range:

$$N \geq \frac{V_{OUT_sec} + R_{wind_sec} \cdot I_{OUT_sec} + V_{FD1}}{V_{OUT_pri} + I_{OUT_pri} \cdot (R_{DS(on)LS} + R_{wind_pri})} \quad (38)$$

If no current is drawn from the primary output, the turn ratio should only be chosen to compensate the drops due to the secondary winding resistance and the Schottky diode.

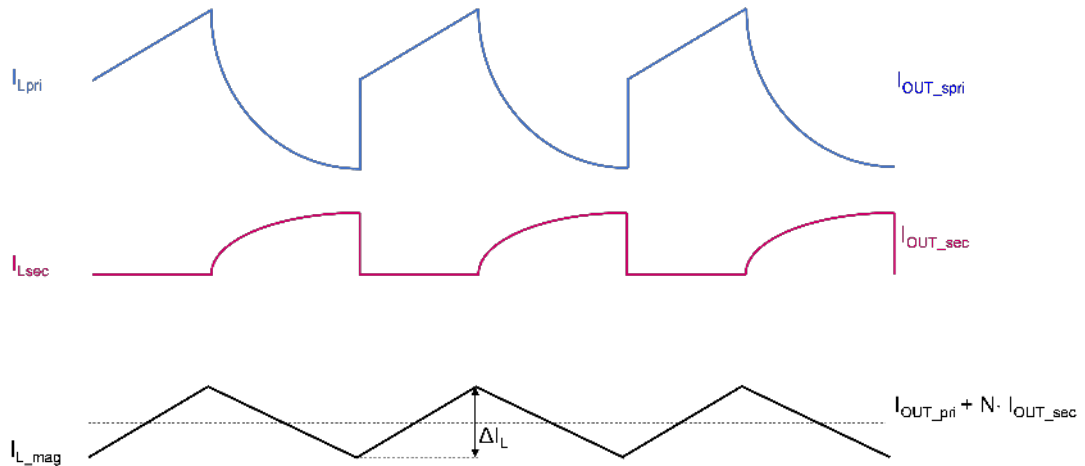
The effect of the leakage inductance on the secondary output voltage regulation (not included in the equation above) should be taken into account too. Figure 17 clearly shows how the secondary output voltage can drift due to the leakage inductance.

Primary inductance

The choice of the primary inductance does not differ so much from a standard buck. The magnetizing current, (see Figure 44) which combines the two winding currents, has the same shape as the buck inductor current and can be defined as:

$$I_{L_mag} = I_{pri} + N \cdot I_{sec} \quad (39)$$

Figure 44. Primary winding current (blue), secondary winding current (magenta) and magnetizing current (black)



Therefore, setting the current ripple ΔI_L , the inductance is so defined:

$$L_{pri} = \frac{(V_{IN} - V_{OUT_pri}) \cdot V_{OUT_pri}}{V_{IN} \cdot f_{SW} \cdot \Delta I_L} \quad (40)$$

For example, assuming $I_{OUT_prim} = 500$ mA, $I_{OUT_sec} = 100$ mA, $N = 6$, the current ripple can be set around 30% of the total current $I_{OUT_pri} + N \cdot I_{OUT_sec} = 1.1$ A, therefore, 330 mA. If $V_{IN} = 12$ V, $V_{OUT_pri} = 5$ V and $f_{SW} = 400$ kHz, the inductor value should be 22 μ H.

Peak and RMS current

As any inductor, peak and RMS current for each winding must be calculated in order to define saturation and RMS currents that the transformer should fulfill.

For the primary winding, the equations below are valid:

$$I_{pri_pos_peak} = I_{OUT_pri} + \frac{I_{OUT_sec}}{N} + \frac{\Delta I_{pri}}{2} \quad (41)$$

$$I_{pri_RMS} = \left(I_{OUT_pri} + \frac{I_{OUT_sec}}{N} \right) \cdot \sqrt{1 + \frac{1}{12} \cdot \left(\frac{\Delta I_{pri} \cdot N}{N \cdot I_{OUT_pri} + I_{OUT_sec}} \right)^2} \quad (42)$$

For the secondary winding, the peak current can change depending on the leakage inductance. In the image below secondary winding current waveforms with different leakage inductances are simulated. It is evident how the peak current can significantly vary. Considering the target leakage inductance value for an iso-buck (recommended up to 1% of the primary inductance), the waveform can be approximated with a sawtooth shape and the peak and RMS currents can be hence estimated as:

$$I_{sec_pos_peak} = \frac{2 \cdot I_{OUT_sec}}{1-D} \quad (43)$$

$$I_{sec_RMS} = I_{sec_pos_peak} \cdot \sqrt{\frac{1-D}{3}} \quad (44)$$

Eq. (43) gives an indication of the peak value. Nevertheless, the waveform can significantly change with the leakage. Therefore, the measured peak value can differ from the one provided by this equation.

A duty cycle higher than 50-60 % significantly increases the peak current in the secondary winding, therefore affecting the negative peak current at the primary side.

Windings resistance

Winding resistances should be minimized as much as possible since they affect the secondary output load regulations. They also contribute to power losses, and so affect the efficiency of the total solution.

Leakage inductance

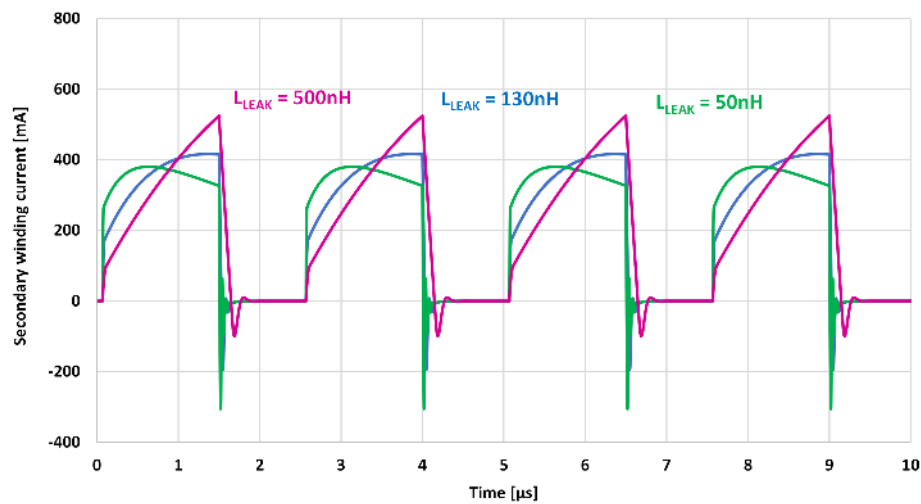
The leakage inductance of a transformer can be defined as an undesired inductive component due to the not perfect magnetic linking of the two windings. Leakage inductance is inherent to the transformer construction and can only be reduced but not eliminated.

As shown in [Figure 45](#), the leakage inductance affects the shape of the secondary winding current. In general, a very low leakage inductance implies that the current in the secondary winding can quickly ramp up, allowing the charge of the secondary output capacitor and supporting the load current demand.

A high leakage inductance slows down the secondary winding current rise, limiting the charge delivery to the output. Comparing solutions with different values of transformer leakage inductance shows that higher leakage inductance transformers are characterized by poorer load regulation performances (as already depicted in [Figure 22](#)).

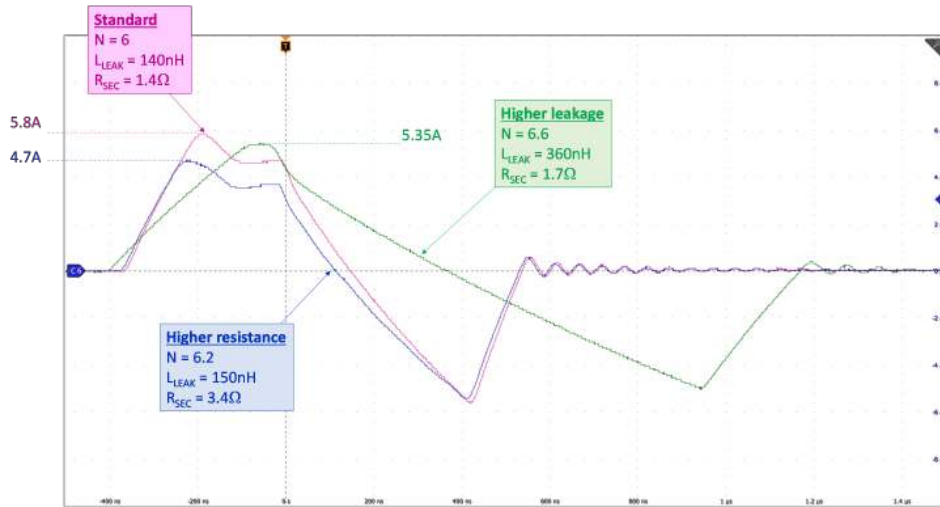
On the other hand, the leakage inductance determines the slope of the rising edge of current in the primary winding (the lower the leakage, the steeper the slope) and the peak value it could reach. Therefore, under certain conditions (for example short-circuit at the secondary side) this peak can be significantly high.

Figure 45. Impact of the leakage inductance on the secondary winding peak current



A higher value of the leakage can help in these cases, jeopardizing however the load regulation performances. A similar effect can be also achieved by increasing the resistance of the secondary winding, keeping the optimized value of the inductance. In both cases it is also possible to adjust the N value to improve the load regulation (see [Figure 46](#)). Both higher leakage and higher secondary winding resistance have a slight negative impact on the efficiency.

Figure 46. Primary winding current peak reduction with higher leakage or higher secondary winding resistance

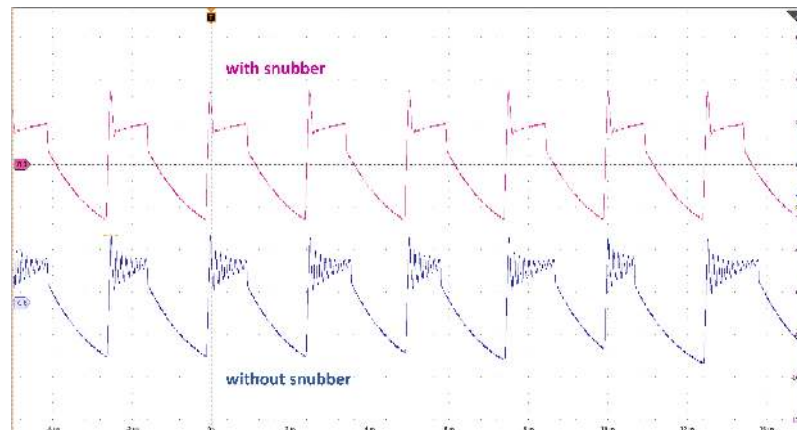


Another effect of the leakage inductance is the ringing observed when the transition from the off-phase to on-phase occurs. These oscillations are due to the LC circuit represented by the leakage inductance and the total parasitic capacitance observed by the primary winding. This capacitance consists of several contributions:

- Primary winding capacitance
- Secondary winding capacitance, reflected to the primary side
- Reverse capacitance of the Schottky diode, reflected to the primary side

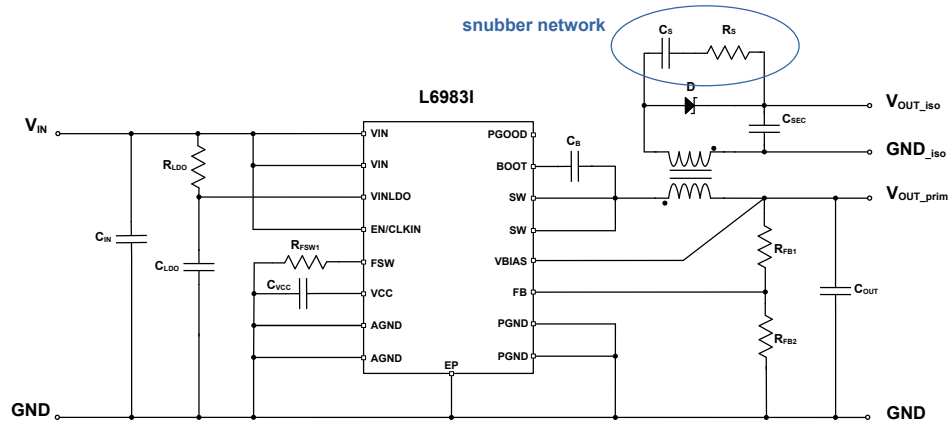
The ringing at primary side could affect the regulation loop and falsely trigger the internal comparator, turning off the high-side MOSFET although it should be kept on. This might result in undesired jitter at switch node.

Figure 47. Filtering effect of the snubber network



A proper masking time ($T_{ON\ MIN}$) filters these oscillations, which otherwise can affect the loop on the primary side. Nevertheless, an RC snubber circuit (depicted in [Figure 48. RC snubber network](#)) to dump this ringing is always recommended.

Figure 48. RC snubber network

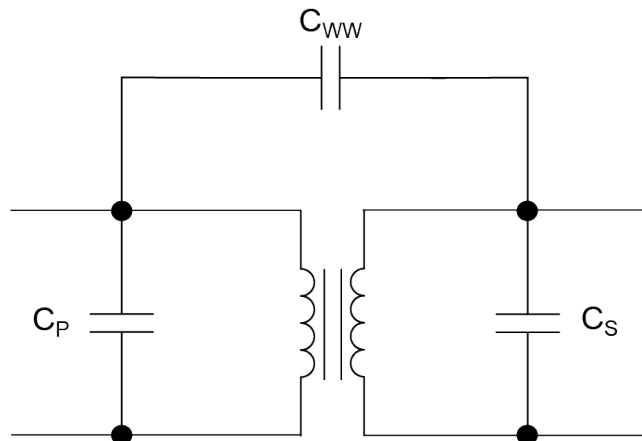


Capacitance

The parasitic capacitance of a real transformer mainly consists of the following contributions:

- Capacitance across each winding (C_P and C_S , in the image below) due to the capacitive coupling between the coil and the core. As already mentioned, the winding capacitances are involved in the ringing observed during transition from off to on-phase of the primary side.
- Interwinding capacitance (C_{WW}), that is the capacitance between windings. The interwinding capacitance should be reduced in order to limit disturbance on the primary side due to possible steep voltage transitions present in the load connected to the secondary output.

Figure 49. Transformer parasitic capacitances



10.3 Schottky diode

In the selection of the Schottky diode, the following parameters should be considered:

- Maximum forward current, mainly defined by the secondary output current demand (see Eq. (44))
- Forward voltage drop, which affects the secondary output voltage regulation
- Maximum peak reverse voltage. During the on-phase of the primary side, when in the secondary side no current flows, the diode is reverse biased and must withstand this voltage:

$$V_{D1_rev} = N \cdot (V_{INmax} - V_{OUT_pri}) + V_{OUT_sec} \tag{45}$$

- Junction capacitance, which should be as low as possible in order to reduce the ringing described in the previous section

10.4 Output capacitors selection

Primary output capacitor

As in a standard buck converter, the primary output capacitor is involved in:

- Determining the output voltage ripple
- Supporting load transient
- Loop stability, by setting one pole and one zero in the transfer function

Considering the output voltage ripple requirement, the primary output capacitance should be selected according to the following equation:

$$C_{OUT_pri} = \frac{\Delta I_{pri}}{8 \cdot f_{SW} \cdot (\Delta V_{OUT_pri} - ESR \cdot \Delta I_{pri})} \quad (46)$$

Normally, MLCC capacitors are the best choice for the output capacitor, therefore the ESR contribution is negligible and Eq. (46) can be simplified.

Secondary output capacitor

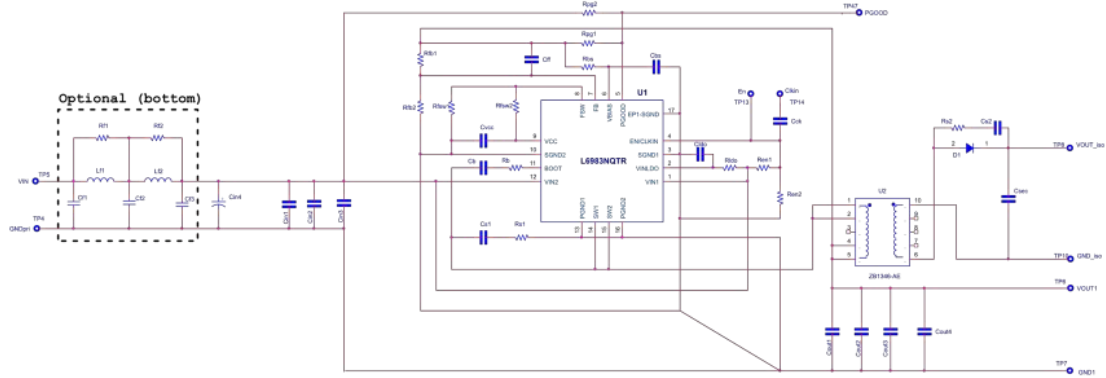
The secondary output capacitor supplies the secondary output load current during the t_{ON} (when diode D1 is reverse biased) and its value defines the secondary output voltage ripple (ΔV_{OUT}).

$$C_{OUT_sec} = \frac{I_{OUT_sec} \cdot D}{\Delta V_{OUT_sec} \cdot f_{SW}} \quad (47)$$

11 Application board

The application board (STEVAL-L6983IV1) schematic is shown in the figure below.

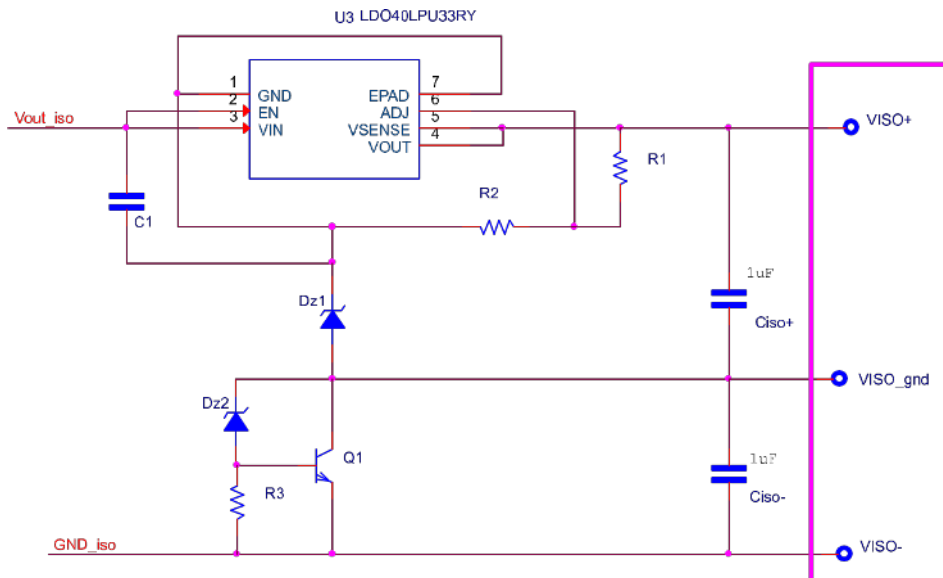
Figure 50. Schematic of the application board (unregulated isolated output)



The additional input filter (in the dotted box in Figure 50, on the bottom side of the board) limits the conducted emission on the power supply. In case the filter is not necessary or should be bypassed for any test, two 0 Ω resistors should be placed at Rf1 and Rf2.

The isolated output supplied by the board is unregulated. Nevertheless, a post-regulation circuit (see schematic in Figure 51) is provided on the bottom side (components not mounted). The values and the components indicated in the BOM below (Table 9) are assumed for a dual voltage 18 V / - 5 V.

Figure 51. Proposed circuitry for post-regulation (not mounted, bottom side) for dual voltage (18 V / - 5 V)



If a different dual isolated voltage is necessary (for example, 15 V / - 6 V), the replacement of two components is enough to adapt the board: the Zener diode D_{Z2} (with a diode providing the most suitable Zener voltage) and the resistor divider (one of the two resistors) R₁-R₂, in accordance with the equation:

$$V_{ISO+} = 1.2V \cdot \frac{R_1 + R_2}{R_2} + V_{DZ1} \quad (48)$$

Table 9. BOM

Reference	Part number	Description	Value	Manufacturer
U1	L6983NQTR			ST
U2	ZB1346-AE	Transformer	N = 6, 2 kV isolation	Coilcraft
Rs1		0805 SMD resistor	Not mounted	
Rs2		0805 SMD resistor	300 Ω	
Rb		0603 SMD resistor	0 Ω	
Ren1		0603 SMD resistor	100 k Ω	
Ren2		0603 SMD resistor	Not mounted	
Rfb1		0603 SMD resistor	360 k Ω	
Rfb2		0603 SMD resistor	75 k Ω	
Rfsw1		0603 SMD resistor	0 Ω	
Rfsw2		0603 SMD resistor	Not mounted	
Rpg1		0603 SMD resistor	Not mounted	
Rpg2		0603 SMD resistor	Not mounted	
Rbs		0603 SMD resistor	0 Ω	
Rldo		0603 SMD resistor	100 Ω	
Clido		0603 MLCC	1 μ F, 50 V	
Cff		0603 MLCC	Not mounted	
Cbs		0603 MLCC	100 nF, 50 V	
Cs1		0603 MLCC	Not mounted	
Cs2		0603 MLCC	180 pF, 50 V	
Cin1		1206 MLCC	10 μ F, 50 V	
Cin2, Cin3		0805 MLCC	1 μ F, 50 V	
Cin4		SMD electrolytic capacitor, 10x10 mm	100 μ F, 50 V	Panasonic
Cout, Cout2, Cout3		1206 MLCC	22 μ F, 50 V	
Cout4		0603 MLCC	Not mounted	
Csec		1206 MLCC	22 μ F, 50 V	
Cck		0603 MLCC	Not mounted	
Cbs		0603 MLCC	Not mounted	
D1	STPS1170AY	Schottky diode	$V_{RRM} = 170$ V, $I_F = 1$ A	ST
EMI input filter				
Rf1		0603/0805 SMD resistor		
Rf2		0603/0805 SMD resistor		
Cf1, Cf2, Cf3		1206 MLCC, 4.7 μ F, 50 V		
Lf1	MPZ2012S221A	220 Ω Ferrite bead, 100 MHz		
Lf2	XGL4030-682ME	6.8 μ H coil		Coilcraft
Post regulation circuitry (option 18 V/-5 V)				
U3		LDO	Not mounted (DFN6)	ST
R1		0603 SMD resistor	Not mounted (910 Ω)	
R2		0603 SMD resistor	Not mounted (220 Ω)	

Reference	Part number	Description	Value	Manufacturer
R3		0603 SMD resistor	Not mounted (330 Ω)	
C1		0603 MLCC	Not mounted (1 μ F, 35 V)	
Ciso+, Ciso-		0805 MLCC	Not mounted (1 μ F, 50 V)	
Dz1		Zener diode	Not mounted (Vz1 = 12 V)	
Dz2		4.7 V Zener diode	Not mounted (Vz1 = 4.7 V)	
Q1	2STR1215	NPN power transistor	Not mounted	ST

Figure 52. STEVAL-L6983IV1 (top layer)

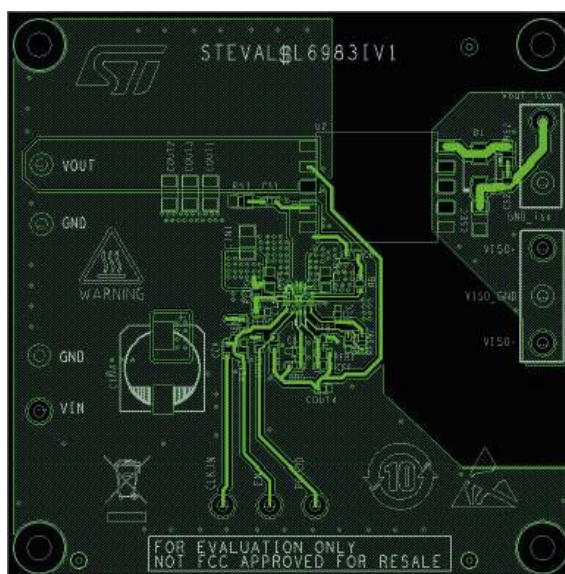
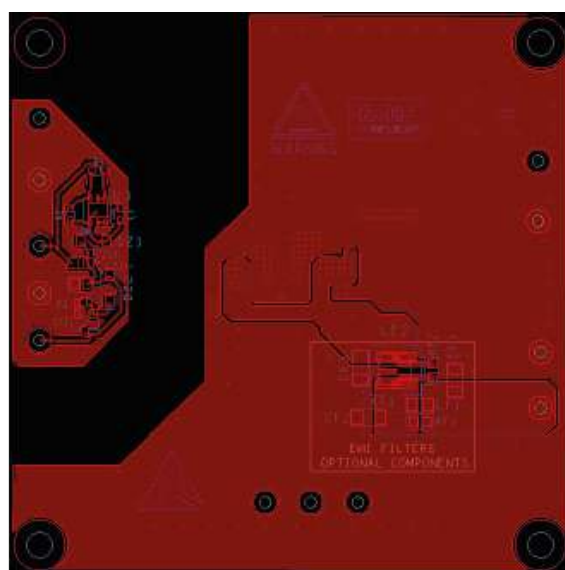


Figure 53. STEVAL-L6983IV1 (bottom layer)



12 Package information

In order to meet environmental requirements, ST offers these devices in different grades of **ECOPACK** packages, depending on their level of environmental compliance. ECOPACK specifications, grade definitions and product status are available at: www.st.com. ECOPACK is an ST trademark.

12.1 QFN16 (3x3 mm) package information

Figure 54. QFN16 (3x3 mm) package outline

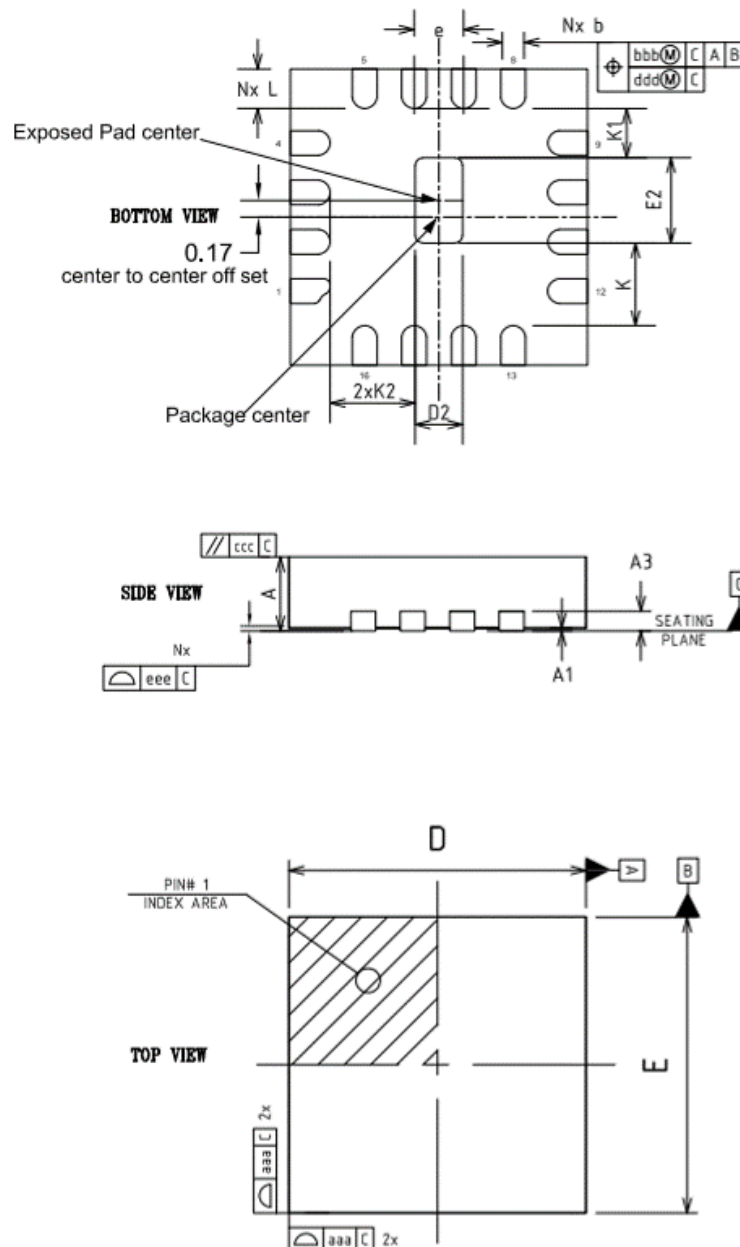
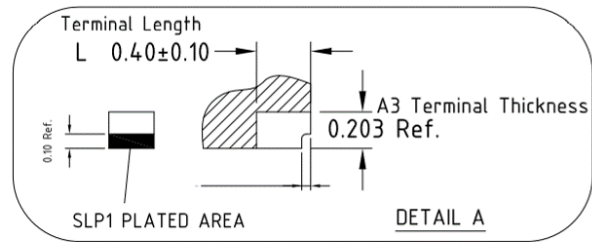
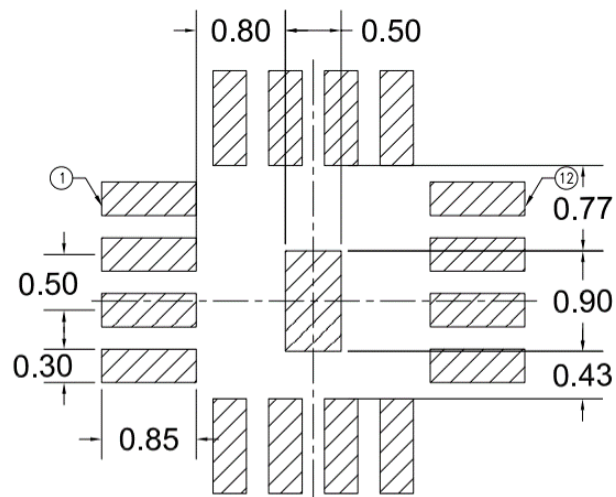


Figure 55. QFN16 (3x3mm) package outline. Detail A

Table 10. QFN16 (3x3mm) mechanical data

Symbol	mm		
	Min.	Typ.	Max.
A	0.7	0.75	0.8
A1	0		0.05
A2	0,5	0.55	0.6
A3	0,203REEF		
b	0.2	0.25	0.3
L	0.3	0.4	0.5
e	0,50BSC		
D	2,95	3	3,05
E	2,95	3	3,05
D1	0,43	0,48	0,53
E1	0.81	0,86	0,91

Figure 56. QFN16 (3x3 mm) recommended footprint


13 Ordering information

Table 11. Order code

Part number	Package	Packing
L6983IQTR	QFN16	Tape and reel

Revision history

Table 12. Document revision history

Date	Revision	Changes
04-Oct-2022	1	Initial release.

Contents

1	Pin configuration	2
2	Typical application circuit	4
3	Maximum ratings	5
3.1	Absolute maximum ratings	5
3.2	ESD protection	5
3.3	Thermal characteristics	5
4	Electrical characteristics	6
4.1	Frequency selection table	8
5	Functional description	9
5.1	Primary side	9
5.1.1	Enable	10
5.1.2	Soft-start	11
5.1.3	Undervoltage lockout	12
5.1.4	Minimum on-time	13
5.1.5	Switch-over feature	14
5.1.6	Spread spectrum	14
5.2	Transformer	15
5.3	Secondary side	15
5.4	Iso-buck operation principle	16
6	Iso-buck performances	17
6.1	Output voltage line regulation	17
6.2	Output voltage load regulation	19
6.3	Efficiency	20
7	Device protections	23
7.1	Overvoltage protection	23
7.2	Overcurrent protection	23
7.3	Thermal shutdown	25
7.4	Power good	25
8	Closing the loop	27
8.1	$G_{CO(s)}$ control to output transfer function	27
8.2	Error amplifier compensation network	28
8.3	Voltage divider	29
9	Application notes	31
9.1	Output voltage adjustment	31

9.2	Switching frequency	33
9.3	Programmable power-up threshold.....	33
9.4	Output External synchronization	34
10	Design of the external components	36
10.1	Input capacitor selection.....	36
10.2	Transformer selection	38
10.3	Schottky diode	42
10.4	Output capacitors selection	43
11	Application board.....	44
12	Package information.....	47
12.1	QFN16 (3x3 mm) package information.....	47
13	Ordering information	49
	Revision history	50

List of tables

Table 1.	Pin description	2
Table 2.	Typical application component	4
Table 3.	Absolute maximum ratings	5
Table 4.	ESD performance	5
Table 5.	Thermal data	5
Table 6.	Electrical characteristics	6
Table 7.	FSW selection	8
Table 8.	External synchronization AC coupling suggested operation range	35
Table 9.	BOM	45
Table 10.	QFN16 (3x3mm) mechanical data	48
Table 11.	Order code	49
Table 12.	Document revision history	50

List of figures

Figure 1.	Pin connection (top view)	2
Figure 2.	Basic application	4
Figure 3.	Frequency setting with dithering (left) and without (right)	8
Figure 4.	Iso-buck general schematic	9
Figure 5.	Block diagram	10
Figure 6.	Power-up/down procedure	11
Figure 7.	Soft-start procedure	12
Figure 8.	Tracked soft-start at secondary side	12
Figure 9.	Simulation with different masking times: insufficient (< 100 ns, left) and appropriate (390 ns, right)	13
Figure 10.	Remaining oscillations (left) and their filtering with RC snubber (right) $V_{IN} = 12\text{ V}$, $N = 6$, $I_{OUT_{iso}} = 200\text{ mA}$	13
Figure 11.	Switch-over selection.	14
Figure 12.	Effect of the switch-over on the efficiency for primary output (left) and isolated secondary output (right)	14
Figure 13.	Switching frequency trend with spread spectrum feature activated.	15
Figure 14.	Iso-buck basic operating principle	16
Figure 15.	Iso-buck primary and secondary current waveforms	16
Figure 16.	Reference schematic for measurements of line and load regulation and efficiency.	17
Figure 17.	Primary output line regulation ($V_{OUT_{prim}} = 5\text{ V}$, $f_{SW} = 400\text{ kHz}$)	17
Figure 18.	Secondary output line regulation ($V_{OUT_{prim}} = 5\text{ V}$, $f_{SW} = 400\text{ kHz}$, $N = 6$)	18
Figure 19.	Secondary winding current at different input voltages.	18
Figure 20.	Load regulation of the primary not isolated output voltage ($V_{IN} = 12\text{ V}$, $V_{OUT_{prim}} = 5\text{ V}$, $f_{SW} = 400\text{ kHz}$)	19
Figure 21.	Load regulation of the secondary isolated output voltage ($V_{IN} = 12\text{ V}$, $V_{OUT_{prim}} = 5\text{ V}$, $f_{SW} = 400\text{ kHz}$, $N = 6$)	19
Figure 22.	Effect of the transformer leakage inductance on the isolated output load regulation ($V_{IN} = 12\text{ V}$, $V_{OUT_{prim}} = 5\text{ V}$, $N = 6$)	20
Figure 23.	Primary output efficiency ($V_{OUT_{prim}} = 5\text{ V}$, $f_{SW} = 400\text{ kHz}$, secondary isolated output not loaded)	20
Figure 24.	Primary output efficiency vs. switching frequency ($V_{IN} = 12\text{ V}$, $V_{OUT_{prim}} = 5\text{ V}$, secondary isolated output (not loaded)	21
Figure 25.	Secondary isolated output efficiency at different input voltages ($V_{OUT_{prim}} = 5\text{ V}$, $f_{SW} = 400\text{ kHz}$, $N = 6$)	21
Figure 26.	Secondary output efficiency vs. switching frequency ($V_{IN} = 12\text{ V}$, $V_{OUT_{prim}} = 5\text{ V}$, $N = 6$)	22
Figure 27.	Isolated output voltage ripple vs. switching frequency ($C_{OUT_{iso}} = 10\text{ }\mu\text{F}$)	22
Figure 28.	Effects of the peak and valley current protections on duty cycle and frequency	23
Figure 29.	Soft-start procedure with short-circuit at the primary output.	24
Figure 30.	Overcurrent procedure in case of persistent short-circuit at the primary output	24
Figure 31.	Peak currents in LS and HS MOSFET depending on the isolated output current ($V_{IN} = 12\text{ V}$, $V_{OUT_{prim}} = 5\text{ V}$, $N = 6$)	25
Figure 32.	Left: $V_{IN} = 12\text{ V}$, I_{PRIM} exceeds I_{VY_SINK} . Right: $V_{IN} = 18\text{ V}$, I_{PRIM} exceeds I_{PK}	25
Figure 33.	PGOOD thresholds	26
Figure 34.	Block diagram of the loop.	27
Figure 35.	Transconductance embedded error amplifier	28
Figure 36.	Contribution of the resistor divider	29
Figure 37.	Primary output voltage regulation	31
Figure 38.	Isolated voltage variation due to the primary output current	32
Figure 39.	Secondary output maximum current	32
Figure 40.	Programming power-up threshold	33
Figure 41.	External synchronization (direct connection)	34
Figure 42.	External synchronization (AC coupling)	35
Figure 43.	Input capacitor AC current	36
Figure 44.	Primary winding current (blue), secondary winding current (magenta) and magnetizing current (black)	39
Figure 45.	Impact of the leakage inductance on the secondary winding peak current	40
Figure 46.	Primary winding current peak reduction with higher leakage or higher secondary winding resistance	41
Figure 47.	Filtering effect of the snubber network	41
Figure 48.	RC snubber network	42
Figure 49.	Transformer parasitic capacitances	42

Figure 50.	Schematic of the application board (unregulated isolated output)	44
Figure 51.	Proposed circuitry for post-regulation (not mounted, bottom side) for dual voltage (18 V / - 5 V)	44
Figure 52.	STEVAL-L6983IV1 (top layer)	46
Figure 53.	STEVAL-L6983IV1 (bottom layer)	46
Figure 54.	QFN16 (3x3 mm) package outline	47
Figure 55.	QFN16 (3x3mm) package outline. Detail A.	48
Figure 56.	QFN16 (3x3 mm) recommended footprint	48

IMPORTANT NOTICE – READ CAREFULLY

STMicroelectronics NV and its subsidiaries (“ST”) reserve the right to make changes, corrections, enhancements, modifications, and improvements to ST products and/or to this document at any time without notice. Purchasers should obtain the latest relevant information on ST products before placing orders. ST products are sold pursuant to ST’s terms and conditions of sale in place at the time of order acknowledgment.

Purchasers are solely responsible for the choice, selection, and use of ST products and ST assumes no liability for application assistance or the design of purchasers’ products.

No license, express or implied, to any intellectual property right is granted by ST herein.

Resale of ST products with provisions different from the information set forth herein shall void any warranty granted by ST for such product.

ST and the ST logo are trademarks of ST. For additional information about ST trademarks, refer to www.st.com/trademarks. All other product or service names are the property of their respective owners.

Information in this document supersedes and replaces information previously supplied in any prior versions of this document.

© 2022 STMicroelectronics – All rights reserved